DISLOCATION PATTERNING UNDER INTERNAL AND EXTERNAL STRESSES

By

Mahesh Kumar Sahu

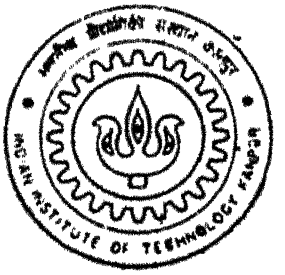

DEPARTMENT OF NUCLEAR ENGG. AND TECH.

Indian Institute of Technology Kanpur

July, 2002

DISLOCATION PATTERNING UNDER INTERNAL AND EXTERNAL STRESSES.

A Thesis Submitted
in Partial Fulfillment of the Requirement
for the Degree of

MASTER OF TECHNOLOGY

By

Mahesh Kumar Sahu

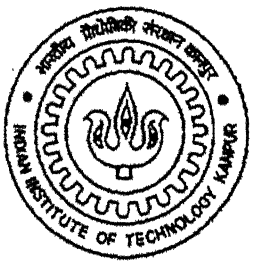

to the

Department of Nuclear Engg. and Tech.

Indian Institute of Technology, Kanpur

July, 2002

CERTIFICATE

It is certified that the work contained in the thesis entitled **"Dislocation Patterning Under Internal and External Stresses "** *by* **Mahesh Kumar Sahu,** *has been carried out under my supervision, and this work has not been submitted elsewhere for a degree.*

Kamal K Kar

Dr. Kamal K.Kar
Assistant Professor
Deptt. of Mech. Engg.
I.I.T. Kanpur

9-7-02

July, 2002

Dedicated to

MY BELOVED TEACHERS

ACKNOWLEDGMENT

I would like to express my deep sense of gratitude to my ever-cherished guide Dr. Vijay B. Shenoy for his invaluable guidance and help throughout my M.Tech. Programme. I am sincerely thankful for his valuable suggestions in my academic as well as personal life.

I am especially thankful to Dr. Kamal K. Kar for his invaluable cooperation and guidance. I am paying my great regards to Dr. M. S. Kalra and Dr. P. Munshi for giving me invaluable exposure to different streams of Nuclear Engg. and Tech. Programme.

I am thankful to Multi-Scale Simulation Lab friends Ashish Gupta, Shivendra Trivedy and Yogesh Kanaujia. My sincere thanks to Kamal Sharma, Gaurav Bhutani and Prashant Dubey for their throughout assistance, amity and company. I wish to thank all my I.I.T. friends for their help in one way or other.

I wish to express my heartful thanks to my friend Atul Sharma and Surya Prakash Dewangan for their endless love, encouragement and endurance which makes my life memorable at I.I.T. Kanpur.

Finally, I am grateful to the Almighty and my family for what I am today.

- Mahesh Kumar Sahu

DISLOCATION PATTERNING UNDER INTERNAL AND EXTERNAL STRESSES

Mahesh Kumar Sahu

SYNOPSIS

Dislocations in one- and two- dimensions have been simulated by a computational technique similar to molecular dynamics. The model employs an array of straight and pure edge dislocations on parallel slip planes. Externally applied stresses and interaction forces due to other dislocations are integrated using a time stepping scheme. In the case of dislocations moving under internal stresses, it is found that the present model reproduces the analytical results accurately. A random two-dimensional array of dislocations found break up into two walls under the action of internal stresses. In addition, these walls become wavy under the action of a cyclic load. These results may be useful in understanding the formation of the persistence slip bands under fatigue loading.

Contents

List of Figures

Nomenclature

u_i : Displacement in i direction.

$\mathbf{u}$: Resultant displacement.

σ_{ij} : Stress vector acting in i direction on j plane .

e_{ij} : Strain vector acting in i direction on j plane .

G : Shear modulus.

λ : Lame constant.

b : Burgers vector.

b_i : Burgers vector's ith component of dislocation.

ν : Poisson's ratio.

$(r\ ,\theta)$:Radial parameters of two-dimensional coordinate.

F : Force acting on dislocation.

τ : Shear stress.

v : Velocity of dislocation.

Δt : Time step of integration.

x_i : x-coordinate of dislocation on step i.

$\sigma 1$:Stress field due to x components of Burgers vector.

$\sigma 2$:Stress field due to y components of Burgers vector.

τ_{ext} : External shear stress.

τ_m : Mean of cyclic stress.

τ_a : Amplitude of cyclic stress.

T : Periodicity of cyclic stress.

x^+ :x-coordinate of positive dislocation.

x^- :x-coordinate of negative dislocation.

x_{min} : Half width of dislocation distribution.

Chapter 1

Introduction

1.1 Introduction

1.1.1 Existence of Dislocations

Although there are many techniques now available for the direct observation of dislocations, the existence of these line defects was deduced by interference in the early stages of dislocation study. Strong evidence arose from attempts to reconcile theoretical and experimental values of the applied shear stress required to *plastically deform* a single crystal. The striking difference between prediction and experimental was accounted for by the presence of dislocations independently by Orawan, Polanyi and Taylor in 1934.

In recent years, it has been possible to produce crystals in the form of fibers of a small diameter, called whiskers, which have a very high degree of perfection. These whiskers are sometimes entirely free of dislocations and there strength is close to the theoretical strength.

Dislocations are mainly divided in two types.

- Edge dislocation
- Screw dislocation

Practically the dislocations are in mixed state of those two types.

1.1.2 Statement of The Problem

The experimental studies of dislocation arrangements in deformed crystals are compromised by the fact that most examinations must be performed *ex post facto.* Consequently such observations cannot address questions of dynamic dislocation interactions and arrangement as functions of dislocation content, character, thermomechanical conditions and crystal geometry. Since few materials are amenable to dynamic observations of dislocations during deformation, *computational modelling* must be employed to determine the nature and geometry of dislocation arrangements under these conditions.

Modelling the evolution of steady-state dislocation arrangements under the action of internal and external stresses is a many-body problem.A complete three-dimensional formulation involves consideration of changes of dislocation shape both within and out of the slip plane as well as appropriate formulation of boundary conditions which do not introduce artifacts into the solutions. Such formulations are limited by the capacity of available computing resources to problems involving relatively few dislocations.

Simulation of dislocation arrangements in two dimensions substantially reduces the computational requirements of the problem while revealing many useful aspects of the evolution of dislocation structure and various thermomechanical conditions. This permits many more variables to be introduced into the problems without incurring an unacceptable penalty in computational requirements. The results of such computations naturally must be interpreted with the simplifications in mind.

Dislocations in deformed metals tend to cluster into various kinds of dense regions of high dislocation density separated by the dislocations of low dislocation density. Observation of dislocation structures in the electron microscope reveals that tend to tangle and to form cells. In worked metals of high stacking fault energies, dislocation are present in planar arrays of high energy, which constitutes a strong driving force for recrystallization.

Low- and high-temperature deformation conditions are defined by the relative importance of glide and climb. Dislocation arrangements resulting from low- and high-temperature deformation exhibit significant differences. At high temperatures dislocations gain an additional degree of freedom through their ability to climb. The

rate of deformation of high-temperatures is primarily controlled by atomic diffusion, which is negligible at low temperatures.After removal of applied stress, dislocations relax into configurations determined by the initial configurations, the relative mobility of glide and climb(We have neglected in our *code*)and the mutual forces among dislocations.

The present study simulates the dislocations both in one-dimensional and two-dimensional.low-temperature condition ,where only glide motion is permitted.Effects of cyclic stresses are also studied.

1.2 Dislocation Theory and Collective Effects

1.2.1 Main Object and Achievement

The main object of dislocation theory is the prediction of the mechanical properties of bulk materials, or at least their understanding, in terms of the physical properties of the material considered and of its structural defects. To date this remains a distant aim despite many detailed studies performed in carefully controlled conditions, in particular on single crystals.

A major achievement of dislocation theory is concerned with the interaction of a mobile dislocation segment with a localized defect which is assumed to be distributed either periodically or at random.The plastic strain rate is obtained by summing up over the total no. of mobile segments the individual properties for cutting through such obstacles, which is equivalent to assume that all events are independent. This leads within a good numerical accuracy to the prediction of the thermal component of the yield stress.

1.2.2 Difference in Local and Average Properties

Models which assume plastic flow to be homogeneous assimilate the local strain rate to the average strain rate and, therefore, identify two quantities which differ by one to two orders of magnitude, at least at moderate strains.

More generally, strain nonuniformities may occur at various scales of observations, macroscopic, mesoscopic(i.e., optical or metallographic) and microscopic.Structural

instabilities can in principle be investigated in terms of dislocation theory, while geometrical instabilities (for instance necking or several types of shear banding) are better described within the framework of micromechanics.
In both cases very basic problems such as the conditions for the occurrence of strain nonuniformities, their scaling laws and the kinetics of their further development are still not well understood.

1.2.3 Dislocation patterning

At moderate and large strains an increasing density of immobile or slow dislocations get stored in the deforming crystals, leading to an increased glide resistance, possibly to long range internal stress and strain hardening. As revealed by transmission electron microscopy these dislocations from various of bi- or three-dimensional arrangements, e.g. wall and channel structures, where dislocation-rich regions alternate more or less regularly with dislocation-poor regions(Louchet and Brechet, 1988; Amodeo, 1988; Hansen and Kuhlmann-Wilsdorf, 1986)
The relation between microstructure and the strain hardening properties of solids has been the object of many phenomenological models. In the simplest ones the dislocation densities are considered and their evolution with time or strain is through a balance between production and storage or annihilation events. More elaborated models assume a particular type of spatial distribution for the mobile and stored dislocations, and consider it as the smallest elementary volume whose mechanical properties are identical to those of the bulk crystal.
The underlying questions, which are still at debate are as follows:

- What are the conditions of occurrence for such type of ordered or semi-ordered microstructures, which we further refer as "pattern"?
- What are the material parameters governing their geometry, their evolution, their transformation during straining ?
- How they may be related to strain hardening properties?

- Is the formation of a field of long range internal stresses necessarily associated with patterning?

1.3 Progress in Dislocation Study

Although this brief description of dislocation theory and of its limitation may seem a bit schematic, the need for a consistent modeling of collective dislocation effects and of their consequences regarding strain hardening and strain localizations has been recognized very early. The tools, both conceptual and numerical, needed to develop such an approach have only been made available in the last two decades through the investigation of the dynamic behavior of ensembles of interacting populations.

The application to dislocation theory was initiated in the mid-eighties and it has yielded a few promising primary results. Only a few idealized situations have been investigated to date and this domain is still in its infancy. The connection between collective dislocation effects and patterning phenomena occurring in other systems brought far from thermodynamic equilibrium is, however , firmly established. It can be illustrated by recent achievements(Brechet, 1987; Lepinoux, 1987; Amodeo, 1988; Schiler, 1989;)

1.4 Research Objectives

The field of dislocation is relatively recent topic for scientists.This stream is opened for many innovations. However numerous studies have been conducted of dislocation arrangements formed under thermomechanical conditions. The dynamic behavior of individual dislocations has been studied theoretically, by computer simulation and experimentally. Some studies based upon automata and molecular dynamics simulations for many dislocations are available. However, these model do not consider the true long-range nature of the dislocation-dislocation interactions, which control many of the features of dislocation microstructures. Also these models restricted to single slip system.

The objects of the research include to understand the characteristics of dislocations

when they are simulated on the basis of conventional ways, like stress field of other dislocations.

1. What will be the final arrangements of dislocations when they will be simulated in resultant stress field of other dislocations?

2. The effects of external stresses on dislocations configurations .

The above 1 and 2 steps can be studied for one- as well as two-dimensional array of dislocations.

1.5 Overview of the Study

This thesis consists of total six chapters.First chapter includes the primarily background of the dislocation, short introduction and objects of this research. Chapter two is containing the very important part: formulation of stress field of edge and screw dislocations.Computational procedure and flow chart is also elaborated in this chapter.In chapter three the one-dimensional simulation is explained with computational and analytical method.The internal stress and externally applied stresses are included for computational steps.Chapter four is similar to chapter three except that this explains the two-dimensional simulation.In chapter five the all important results are included and the graphs are explained.In chapter six results are concluded and scope for future work is pointed out.

1.6 Figures of Dislocations

Many types of dislocations are shown on next two pages:

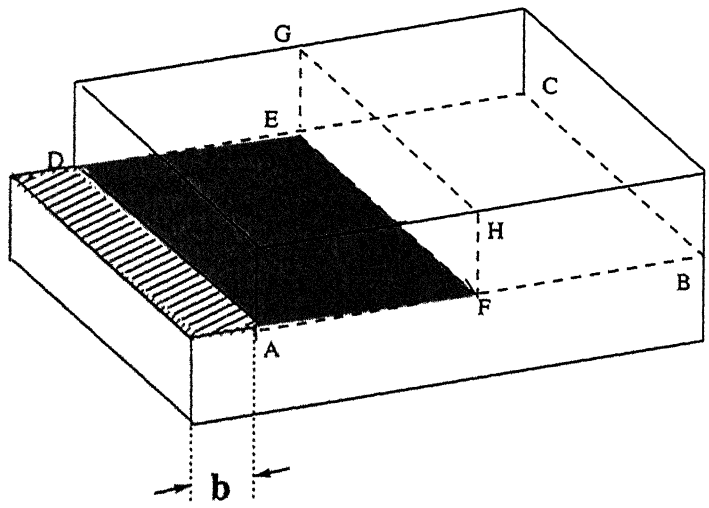

Formation of pure edge dislocation FE.

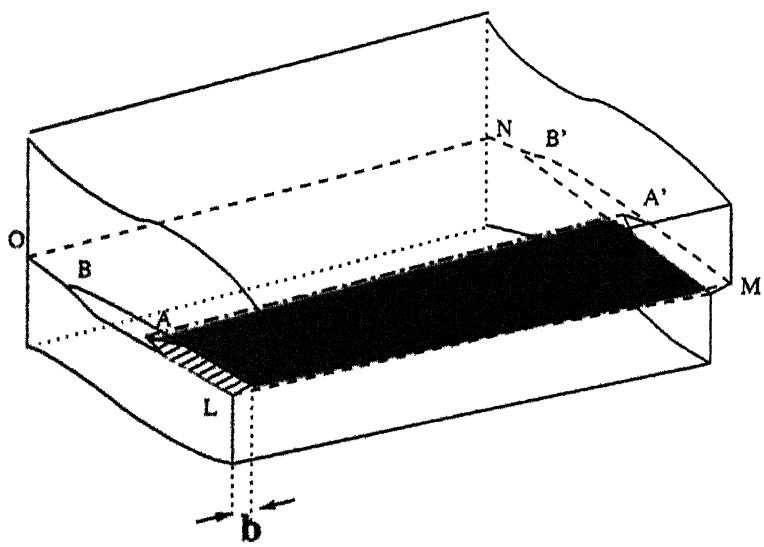

Formation of pure screw dislocation AA'

Figure 1.1: Pure Edge and Pure Screw Dislocations

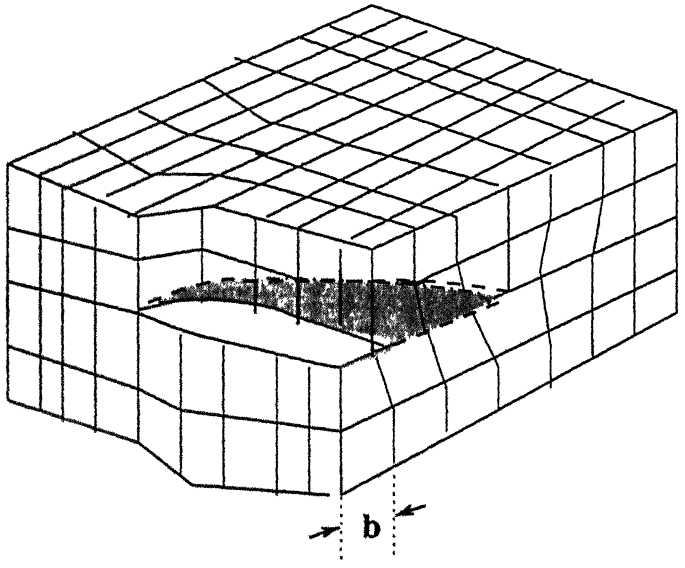

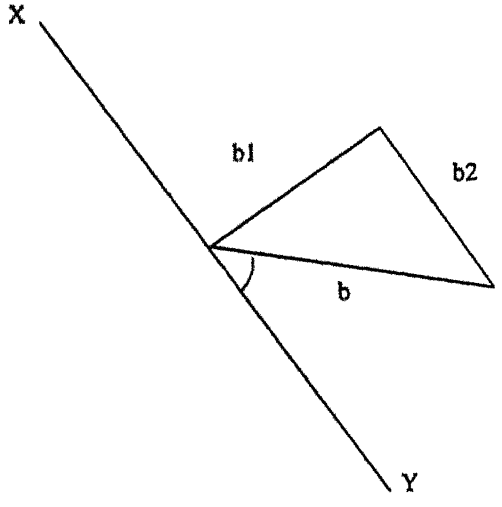

Mixed dislocation:

(a)The curved dislocation SME is pure edge at E and pure screw at S.

(b) Burgers vector b of dislocation XY is resolved into pure edge component b1 and pure screw component b2

Figure 1.2: Mixed Dislocation

Chapter 2

Dislocation Dynamics

2.1 Stress Field of Dislocations

2.1.1 Introduction

The atoms in a crystal containing a dislocation are displaced from their perfect lattice sites, and the resulting distortion produces a stress field in the crystal around the dislocation. The dislocation is therefore a source of *internal stress* in the crystal. The stresses and strains in the bulk of the crystal are sufficiently small for conventional elasticity theory to be applied them. This approach only to be ceases valid at positions very close to the center of the dislocation. Although most crystalline solids are elastically *anisotropic*, it is much simpler to use *isotropic elasticity* theory. This still results in a good approximation in most cases.
From a knowledge of the elastic field, the following important characteristics can be obtained:

- The energy of the dislocation.
- The force it exerts on other dislocations.
- It's energy of interaction with point defects.

The elastic field produced by a dislocation is not affected by the application of stress from *external sources*: the total stress on an element of the body is the superposition of the internal and external stresses.

2.1.2 Elements of Elasticity Theory

The *displacement* of a point in a strained body from its position in the unstrained state is represented by the vector,

$$\mathbf{u} = [u_x, u_y, u_z] \tag{2.1}$$

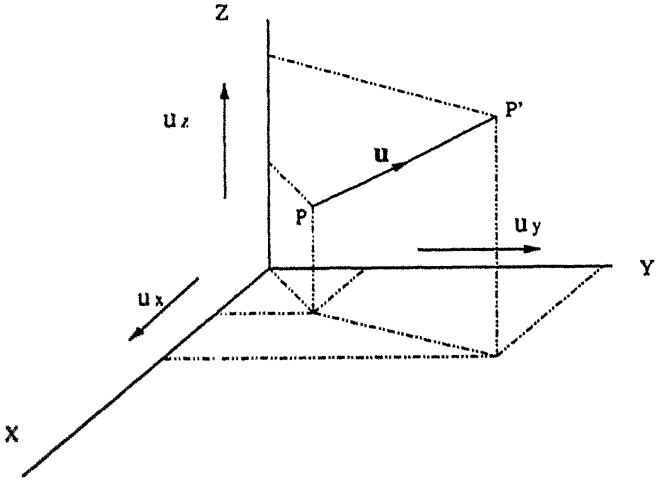

Figure 2.1: Displacement of a point

The components u_x, u_y, u_z represents projections of $\mathbf{u}$ on the x, y, z axes, as shown in Fig. 2.1.In *linear elasticity*, the nine components of *strains* are given in terms of the displacement components thus:

•Normal strains are:

$$e_{xx} = \frac{\partial u_x}{\partial x}, \qquad e_{yy} = \frac{\partial u_y}{\partial y}, \qquad e_{zz} = \frac{\partial u_z}{\partial z} \tag{2.2}$$

•Shear strains are:

$$e_{yz} = e_{zy} = \frac{1}{2}\left(\frac{\partial u_y}{\partial z} + \frac{\partial u_z}{\partial y}\right), \tag{2.3}$$

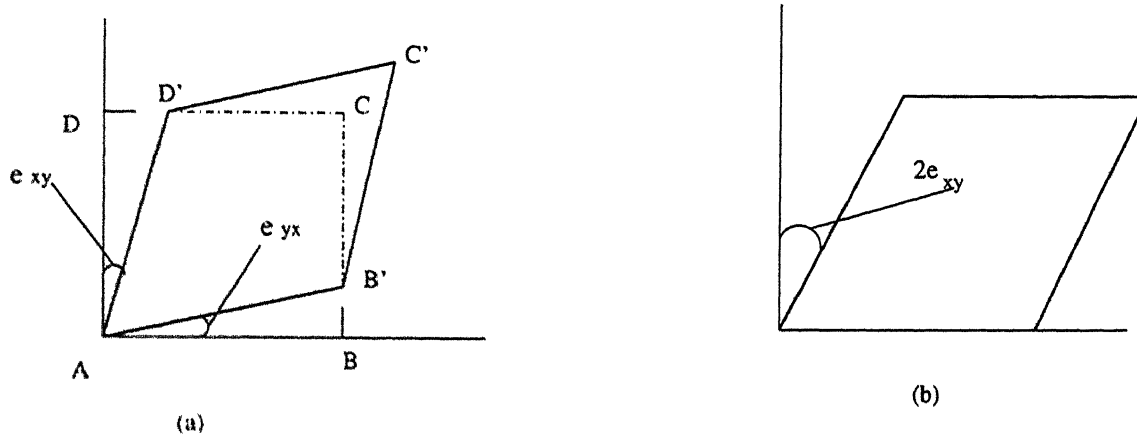

(a)Pure shear and (b)simple shear of an area element in the xy plane.

Figure 2.2: Pure Shear

$$e_{zx} = e_{xz} = \frac{1}{2}\left(\frac{\partial u_z}{\partial x} + \frac{\partial u_x}{\partial z}\right), \tag{2.4}$$

$$e_{yx} = e_{yx} = \frac{1}{2}\left(\frac{\partial u_x}{\partial y} + \frac{\partial u_y}{\partial x}\right) \tag{2.5}$$

Normal strains represent the fractional change in length of elements parallel to the x, y and z axes respectively. *The shear strains* can be understood by the Fig. 2.2(a), in which the small area element $ABCD$ in the xy plane has been strained to the shape $AB'C'D'$ without change of area.The angle between side AB and AD initially parallel to x and y respectively has decreased by $2e_{xy}$. By rotating, but not deforming, the element as in Fig 2.2(b), it is seen that the element has undergone a simple shear. The simple shear often used in engineering practice is $2e_{xy}$, as

icated.

actional change in volume Δ, known as the *dilation*, is therefore:

$$\Delta = \frac{\Delta V}{V} = (e_{xx} + e_{yy} + e_{zz}) \tag{2.6}$$

s independent of the orientation of the axes x,y,z.

elationship between stress and strain in linear elasticity is *Hooke's Law* in

which each stress component is linearly proportional to each strain. For isotropic solids, only two proportionality constants are required:

$$\begin{aligned} \sigma_{xx} &= 2Ge_{xx} + \lambda(e_{xx} + e_{yy} + e_{zz}) \\ \sigma_{yy} &= 2Ge_{yy} + \lambda(e_{xx} + e_{yy} + e_{zz}) \\ \sigma_{zz} &= 2Ge_{zz} + \lambda(e_{xx} + e_{yy} + e_{zz}) \\ \sigma_{xy} = 2Ge_{xy}, \qquad \sigma_{yz} &= 2Ge_{yz}, \qquad \sigma_{zx} = 2Ge_{zx} \end{aligned} \tag{2.7}$$

λ and G are the Lame Constants, but G is more commonly known as the *shear modulus*.

2.1.3 Stress Field of Straight Dislocation

Screw Dislocation:

The elastic field around an infinitely-long, straight dislocation can be represented in terms of a cylinder of elastic material. A radial slit $LMNO$ was cut in the cylinder parallel to the z-axis and the free surfaces displaced rigidly with respect to each other by the distance b,the magnitude of the Burgers vector of the *screw dislocation*, in the z-direction.

The elastic field in the dislocated cylinder can be found by direct inspection. First, it is noted that there are no displacements in the x and y directions:

$$u_x = u_y = o \tag{2.8}$$

Secondly, the displacement in the z direction increases uniformly from zero to b as θ increases from 0 to 2π:

$$u_z = \frac{b\theta}{2\pi} = \frac{b}{2\pi}\tan^{-1}(y/x) \tag{2.9}$$

It is then found from equations (2.2) to (2.5) that

$$e_{xx} = e_{yy} = e_{zz} = e_{xy} = e_{yx} = o$$

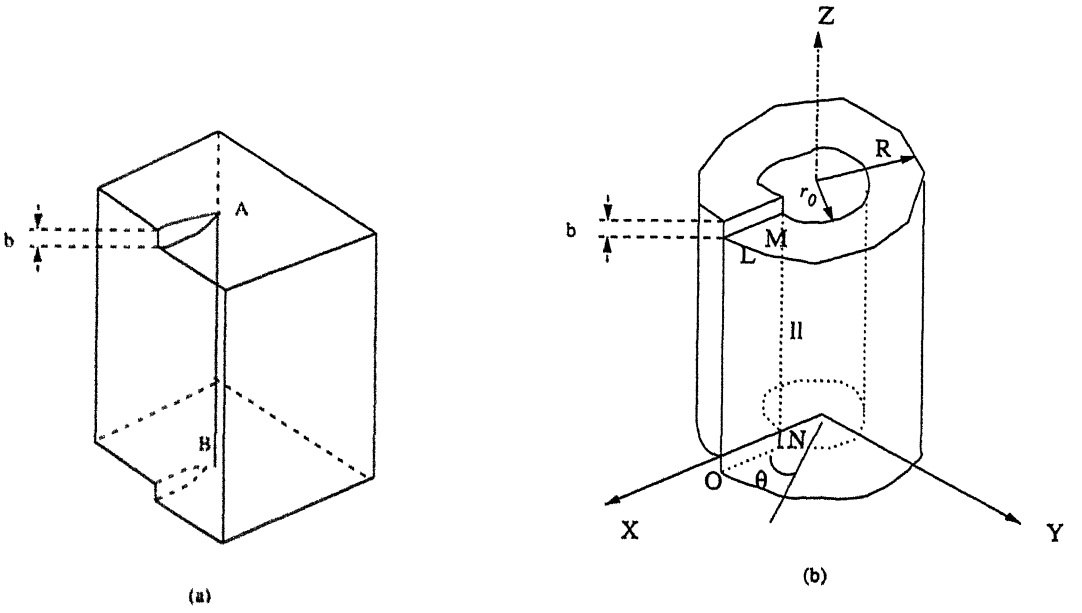

(a) Screw dislocation AB formed in a crystal.

(b) Elastic distortion of a cylidrical ring simulating the distortion produced by the screw dislocation AB.

Figure 2.3: Screw Dislocation

$$e_{xz} = e_{zx} = -\frac{b}{4\pi}\frac{y}{(x^2+y^2)} = -\frac{b}{4\pi}\frac{\sin\theta}{r}$$
$$e_{yz} = e_{zy} = \frac{b}{4\pi}\frac{x}{(x^2+y^2)} = \frac{b}{4\pi}\frac{\cos\theta}{r} \qquad (2.10)$$

From equations (2.7) and (2.10), the components of stresses are

$$\sigma_{xx} = \sigma_{yy} = \sigma_{zz} = \sigma_{xy} = \sigma_{yx} = 0$$
$$\sigma_{xz} = \sigma_{zx} = -\frac{Gb}{2\pi}\frac{y}{(x^2+y^2)} = -\frac{Gb}{2\pi}\frac{\sin\theta}{r}$$
$$\sigma_{yz} = \sigma_{zy} = \frac{Gb}{2\pi}\frac{x}{(x^2+y^2)} = \frac{Gb}{2\pi}\frac{\cos\theta}{r} \qquad (2.11)$$

We can conclude from stress and strain equations (2.10) and (2.11) that:

- The elastic distortion contains no tensile or compressive components and consists of pure shear.
- The stresses and strains are proportional to $1/r$ and therefore diverge to infinity as $r \to 0$. Real crystals are not hollow as taken in this analysis, and so as the center of a dislocation is approached, elasticity theory ceases to be valid and a *non-linear atomistic model* must be used. The region within which the linear elastic solution breaks down is called the *core* of the dislocation.

Edge Dislocation:

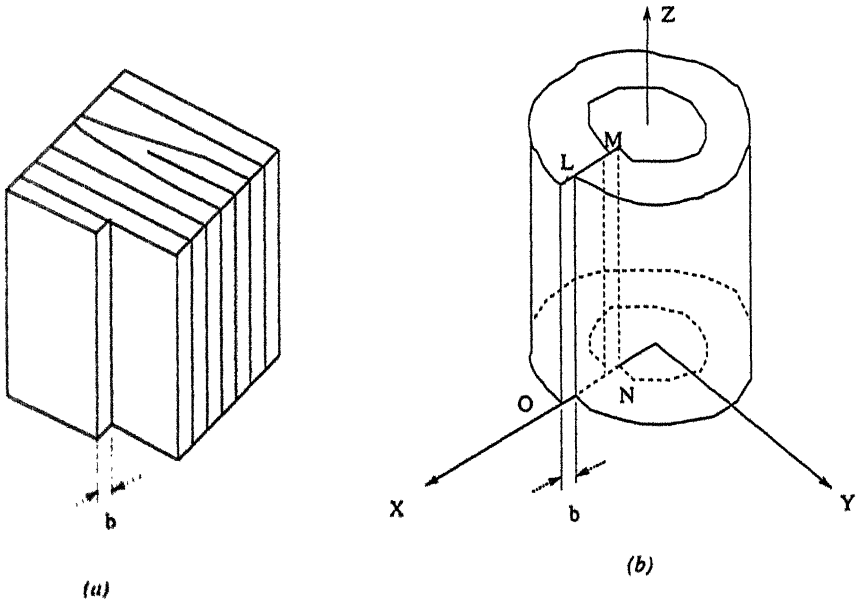

(a)Edge dislocation formed in a crystal .
(b) Elastic distortion of a cylindrical ring simulting the distortion produced by the edge dislocation in (a)

Figure 2.4: Edge Dislocation

The stress field is more complex than that of a screw but can be represented in an isotropic cylinder in a similar way. Considering the edge dislocation in Fig.

2.4(a) elastic strain field can be produced in the cylinder by a displacement of the faces of the slit by a distance b in the x-direction(Fig. 2.4(b)) The stresses are:

$$\sigma_{xx} = -Dy\frac{(3x^2+y^2)}{(x^2+y^2)^2}$$

$$\sigma_{yy} = Dy\frac{(x^2-y^2)}{(x^2+y^2)^2}$$

$$\sigma_{xy} = \sigma_{yx} = Dx\frac{(x^2-y^2)}{(x^2+y^2)^2}$$

$$\sigma_{zz} = \nu(\sigma_{xx}+\sigma_{yy})$$

$$\sigma_{xz} = \sigma_{zx} = \sigma_{yz} = \sigma_{zy} = 0 \tag{2.12}$$

where

$$D = \frac{Gb}{2\pi(1-\nu)}$$

We can say from above equations that:

- The stress field has, therefore, both dilational as well as shear components. The largest normal stress is σ_{xx} which acts parallel to the slip vector.
- The elastic solution has an inverse dependence on distance from the line axis and breaks down when x and y tend to zero. It is valid only outside a core of radius r_0.

2.2 Forces on Dislocations

When a sufficiently high stress is applied to a crystal containing dislocations, the dislocation move and produce plastic deformation either by slip or at sufficiently high temperatures by climb. The load producing the applied stress therefore does work on the crystal when a dislocation moves, and so the dislocation responds to the stress as though it experiences a force equal to the work done divided by the distance it moves. Only glide force is considered here, climb force is neglected.
Consider a dislocation moving in a slip plane under the influence of a uniform resolved shear stress τ (Fig. 2.5). When an element dl of the dislocation line of Burgers vector **b** moves forward a distance ds the crystal plane above and below

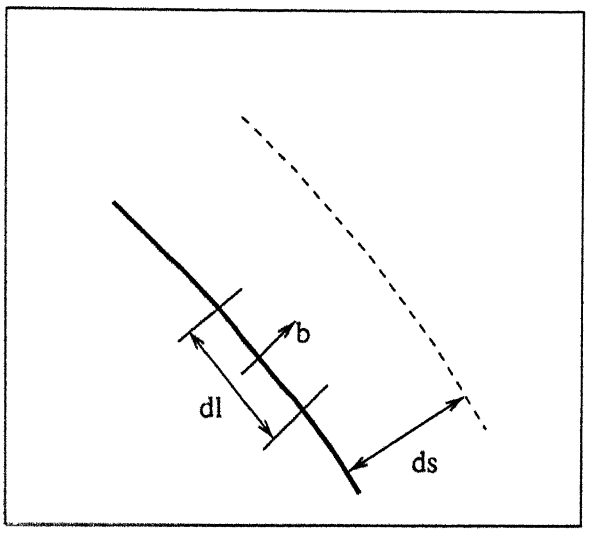

Figure 2.5: Force on Dislocation

the slip plane will be displaced relative to each other by b. The average shear displacement of the crystal surface produced by the glide of dl is:

$$\left(\frac{\mathrm{d}s\mathrm{d}l}{A}\right)b \tag{2.13}$$

Where A is the area of the slip plane. The external force on this area is $A\tau$, so the work done when the element of the slip occurs is

$$dW = A\tau\left(\frac{\mathrm{d}s\mathrm{d}l}{A}\right)b \tag{2.14}$$

the glide force on a unit length of dislocation is defined as the work done when unit length moves unit distance. Therefore,

$$F = \frac{\mathrm{d}W}{\mathrm{d}s\mathrm{d}l} = \frac{\mathrm{d}W}{\mathrm{d}A} = \tau b \tag{2.15}$$

The stress τ is ***the shear stress in the glide plane resolved in the direction of*** $\mathbf{b}$ and the glide force F acts normal to the dislocation at every point along its length.

2.3 Velocity of Dislocation

Dislocations move by glide at velocities which depend on the applied shear stress, purity of crystal, temperature and type of dislocation. A crystal containing freshly introduced dislocations usually produced by lightly deforming the surface, is subjected to constant stress pulse for a given time. From the positions of the dislocations before and after stress pulse, the distance each dislocation has moved, and hence the average dislocation velocity can be determined.
Experimentally the dislocation velocity was measured and observed that dislocation velocity was a very sensitive function of the resolved shear stress.In the range of velocities between 10^{-7} and $10^{-1} cms^{-1}$, the logarithm of the velocity varies linearly with the logarithm of the applied shear stress, mathematically:

$$v \propto \left(\frac{\tau}{\tau_0}\right)^n \tag{2.16}$$

where v is the velocity, τ is the applied shear stress resolved in the slip plane, τ_0 is the shear stress for $v = 1\ cms^{-1}$ and n is a constant and was found experimentally to be ~ 25 for lithium fluoride.It must be emphasized that equation (2.16), is purely empirical and implies no physical interpretation of the mechanism of dislocation motion.

The stress dependence of dislocation velocities varies significantly from one material to another. For a given material, the velocity of transverse shear wave propagation is the limiting velocity for uniform dislocation motion. However damping forces increasingly oppose motion when the velocity increases above about 10^{-3}, and thus n in equation (2.16) decreases rapidly in this range.
Studies on face centered cubic and hexagonal close packed crystals has shown that at the crystal resolved shear stress for macroscopic slip, dislocation velocity is approximately $1ms^{-1}$ (10^{-3} of a shear wave velocity) and satisfies

$$v \propto A\tau^m \tag{2.17}$$

Where A is the material constant and m is approximately 1 at 300 K in pure crystals. We want the relation between velocity of dislocation and force acting on dislocation

for simulation purpose. So we will replace τ in terms of F,

$$v \propto AF/b$$

$$v = \left(\frac{CA}{b}\right)F \tag{2.18}$$

Where C is a proportionality constant. Now we can put all constant terms to unit so that we can get convenient form for simulation, we can write the above equation as:

$$v = F$$

$$\frac{\mathrm{d}x}{\mathrm{d}t} = F \tag{2.19}$$

2.4 Time Integration Scheme

For getting the positions of dislocations on different time steps, difference scheme of *numerical method* can be used. For getting the position after first time step we have to use *forward difference method.*
equation (2.16) can be written in the form of difference:

$$\frac{x_{i+1} - x_i}{\Delta t} = F_i$$

$$x_{i+1} = x_i + \Delta t F_i \tag{2.20}$$

Where x_{i+1} and x_i are the positions of dislocations at $(i+1)$th and ith time steps respectively, Δt is time-step and Fi is the force acting on dislocation at ith time-step.
Now we can use for positions of further time steps with the *central difference method* as that is more accurate than *forward difference method.*

$$\frac{x_{i+1} - x_{i-1}}{2\Delta t} = F_i$$

$$x_{i+1} = x_{i-1} + 2\Delta t F_i \tag{2.21}$$

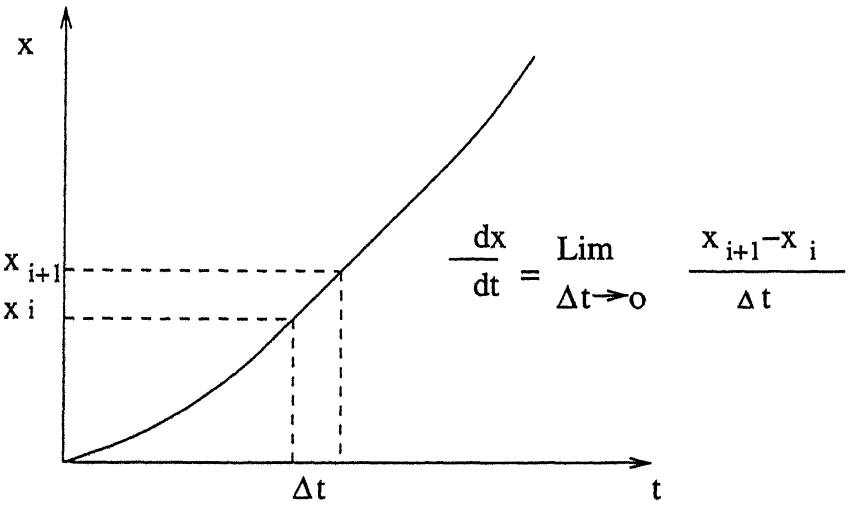

Graphical representation of forward difference method.

Figure 2.6: Difference Method

The equation (2.17) and (2.18) is applicable when Δt is between 0 and 1 and will converge when Δt tends to 0.

2.5 Forces between Dislocations

The basis of the method used to obtain the force between two dislocations is the determination of the additional work done in introducing the second dislocation into the crystal which already contains the first. Consider two dislocations lying parallel to the z-axis. (Fig 2.7).

The total energy of the system consists of:

(a) the self energy of the dislocation I.

(b) the self energy of dislocation II, and

(c) the elastic interaction energy between I and II.

The *interaction energy* E_{int} is the work done in displacing the faces of the cut which creates II in the presence of stress field I. The displacements across the cut are b_x, b_y, b_z the components of the Burgers vector **b** of II. By visualizing the cut parallel

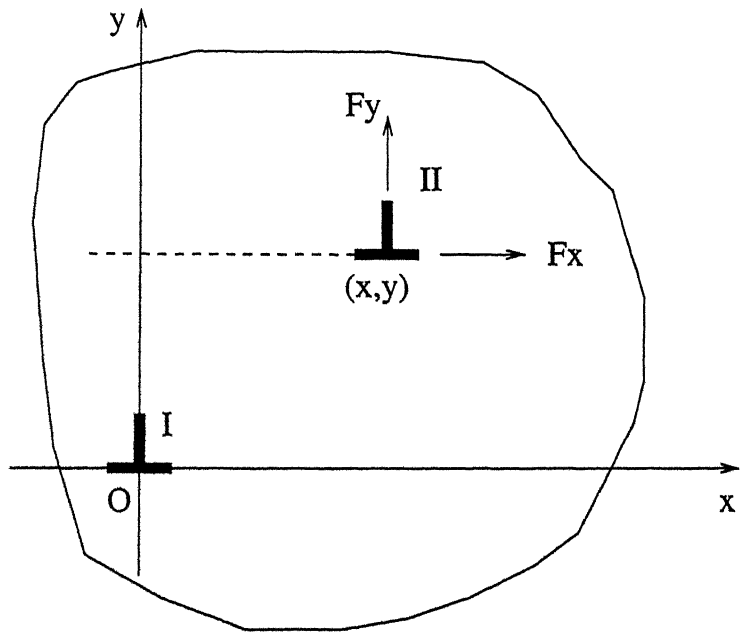

Figure 2.7: Interaction between two edge Dislocations

to the x or y axis, two alternative expressions For E_{int} per unit length of II are

$$E_{int} = \int_x^\infty (b_x\sigma_{xy} + b_y\sigma_{yy} + b_z\sigma_{zy})\mathrm{d}x \tag{2.22}$$

$$E_{int} = \int_y^\infty (b_x\sigma_{xx} + b_y\sigma_{yx} + b_z\sigma_{zx})\mathrm{d}y \tag{2.23}$$

where the stress components are those due to I. The interaction force on II is obtained simply by differentiation of these expressions, i.e. $F_x = -\partial E_{int}/\partial x$ and $F_y = -\partial E_{int}/\partial y$.

For the two parallel edge dislocations with parallel burger vectors shown in Fig. 2.7, $b_y = b_z = 0$ and $b_x = b$, and the components of the force per unit length acting on II are therefore

$$F_x = \sigma_{xy}b, \qquad F_y = \sigma_{xx}b \tag{2.24}$$

where σ_{xy} and σ_{xx} are the stresses of I evaluated at position (x, y) of II. The forces are reversed if II is a negative edge. Equal and opposite forces act on I. F_x is the force

in the glide direction and F_y the force perpendicular to the glide plane. Substituting from equation (2.12) gives

$$F_x = \frac{Gb^2}{2\pi(1-\nu)} \frac{x(x^2-y^2)}{(x^2+y^2)^2} \tag{2.25}$$

$$F_y = \frac{Gb^2}{2\pi(1-\nu)} \frac{y(3x^2+y^2)}{(x^2+y^2)^2} \tag{2.26}$$

Since edge dislocations can move by slip only in the plane contained by the dislocation line and its Burgers vector, the component of the force which is most important in determining the behavior of the dislocations in Fig.2.7 is F_x.

We can conclude from equations (2.25) and (2.26) that:

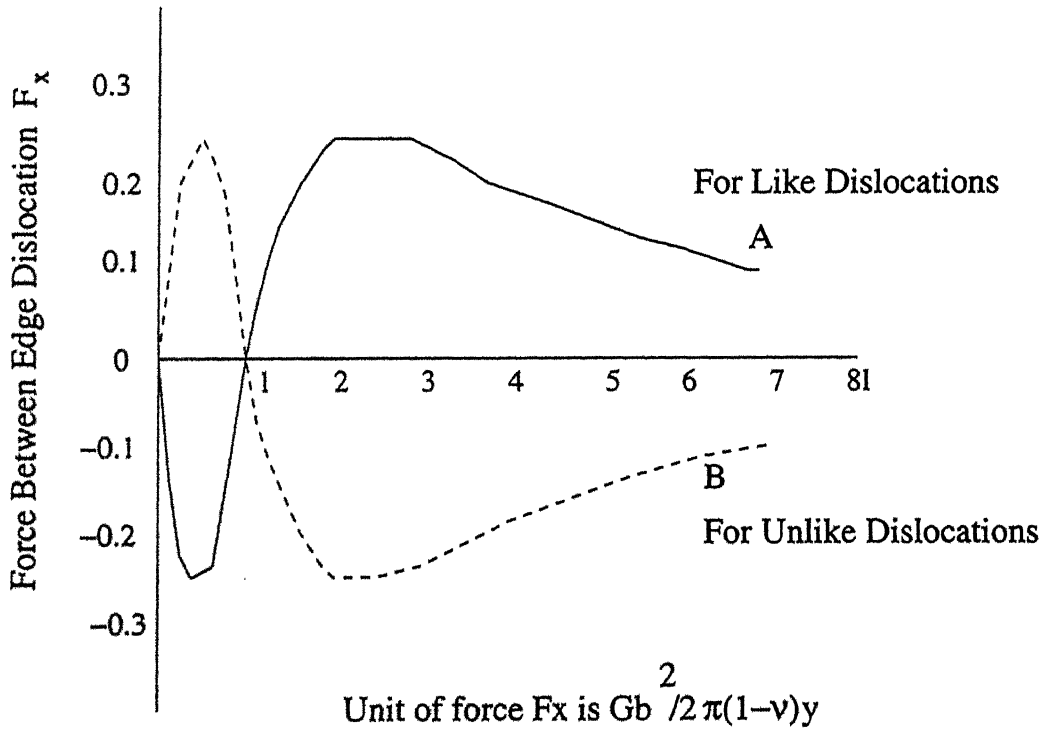

Figure 2.8: Force between parallel edge Dislocations with parallel Burgers vectors.

- for $x > 0, F_x$ is negative (attractive) when $x < y$ for dislocations of same sign
  for dislocations of opposite sign.

- for $x < 0$,F_x is positive (attractive) when $x > -y$ for same sign and $x < -y$ for the opposite sign.

F_x is plotted against x, expressed in units of y, in Fig.2.8. It is 0 when$x = 0, \pm y, \pm\infty$, but of these, the positions of stable equilibrium are seen to be $x = 0, \pm\infty$ for edges of the same sign and $\pm y$ if they have the opposite sign.

It follows that *an array of edge dislocations of the same sign is most stable when the dislocations lie vertically above one another* as in Fig.2.9(a). Furthermore, *edge dislocations of the opposite sign gliding past each other on parallel slip planes tend to form stable dipole* pairs as in Fig. 2.9(b) at low applied stresses.

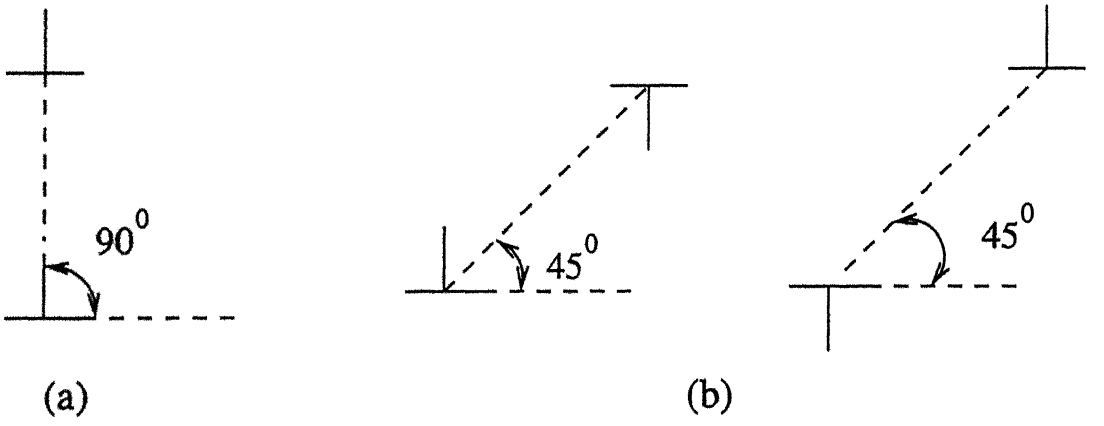

Figure 2.9: Stable positions for two edge dislocations of (a)the same sign and (b) opposite sign.

Comparison of the glide force F_x in equation(2.15) shows that since σ_{xy} is the shear stress in the glide plane of the dislocation II acting in the direction of its Burgers vector, *equation (2.15) holds for both external and internal sources of stress.*

2.6 Unit Dislocation Field

Let a dislocation is placed at (x, y) coordinate and we want the stress field at origin.

in x direction (b_x), is.

$$\sigma 1_{xx} = \frac{-y(3x^2+y^2)}{(x^2+y^2)^2}$$
$$\sigma 1_{yy} = \frac{y(x^2-y^2)}{(x^2+y^2)^2}$$
$$\sigma 1_{xy} = \frac{x(x^2-y^2)}{(x^2+y^2)^2} \tag{2.27}$$

In terms of radial coordinates the above equation can be written as:

$$\sigma 1_{xx} = \frac{\sin\theta(\cos 2\theta + 2)}{r}$$
$$\sigma 1_{yy} = \frac{\sin\theta\cos 2\theta}{r}$$
$$\sigma 1_{xy} = \frac{\cos\theta\cos 2\theta}{r} \tag{2.28}$$

From Fig. 2.10, we can get the stress field for b_y by replacing in $x \rightarrow -y$ and $y \rightarrow x$. So the stress field will be.

$$\sigma 2_{yy} = \frac{-x(3y^2+x^2)}{(x^2+y^2)^2}$$
$$\sigma 2_{xx} = \frac{x(x^2-y^2)}{(x^2+y^2)^2}$$
$$\sigma 2_{yx} = \frac{y(x^2-y^2)}{(x^2+y^2)^2} \tag{2.29}$$

In radial coordinates and in form of $\sigma 1$

$$\sigma 2_{yy} = \frac{\cos\theta(2.0 - \cos 2\theta)}{r}$$

$$\sigma 2_{xx} = \sigma 1_{xy}$$
$$\sigma 2_{yx} = \sigma 1_{yy} \tag{2.30}$$

So the resultant stress field by $\mathbf{b}(b_x, b_y)$:

$$\sigma_{xx} = b_x\sigma 1_{xx} + b_y\sigma 2_{xx}$$

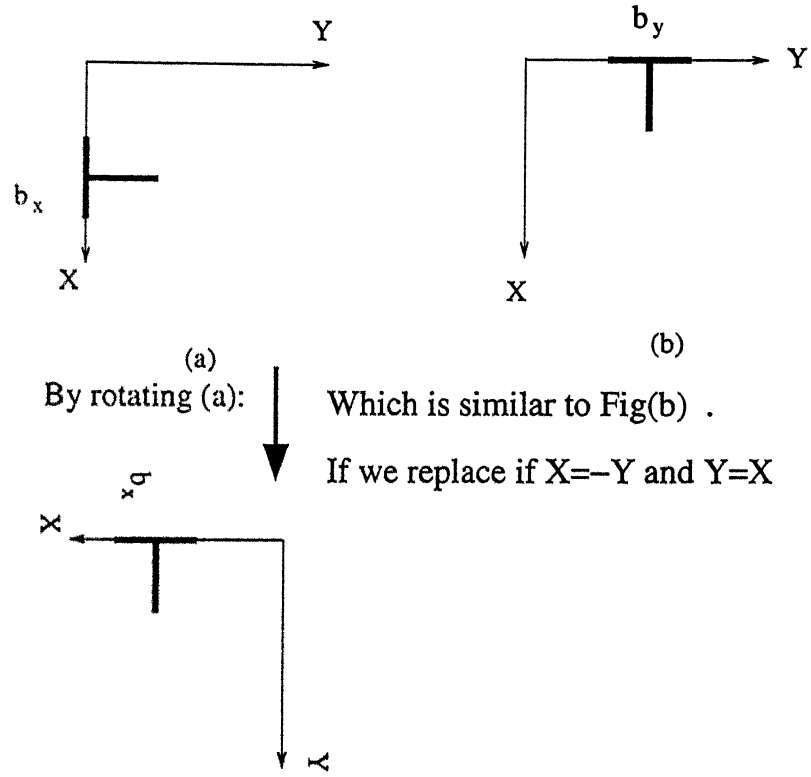

Figure 2.10: Stress Field for Different Orientation.

$$\sigma_{yy} = b_x \sigma 1_{yy} + b_y \sigma 2_{yy}$$
$$\sigma_{xy} = b_x \sigma 1_{xy} + b_y \sigma 2_{xy} \tag{2.31}$$

Let us assume that there are n dislocations for simulation. Each dislocation is influenced by the resultant stress field of all other dislocations. So the expression for force acting on ith dislocation will be (from equation 2.24):

$$F_i = b_i \sum_{j=1}^{n} \tau_{xy}(i,j) \qquad \text{when j} \neq \text{i} \tag{2.32}$$

where $\tau_{xy}(i,j)$ is the stress field of dislocation j on position of ith dislocation, b_i is Burgers vector of ith dislocation and F_i is the force acting on ith dislocation in x direction due to stress field of all other j dislocations.

2.7 Computational Procedure

The specific computational procedures performed by *dislocation simulation code* are explained in following steps:

1. input dislocation parameters like coordinates, Burgers vectors ,time and time-step for simulation. In case of applied stress, parameters of applied stress like periodicity, mean value and amplitude value of stress are also given as input.

2. The total force applied on a single i dislocation by all other j dislocations is calculated.

   - Firstly the distance between dislocations in form of x and y components is calculated and that is got finally in the form of radial parameters (r, θ).
   - From equations (2.28) to (2.31) (from radial distance parameters (r, θ)) the stress field on position of dislocation i is calculated.In case of externally applied shear stress, this stress is simply added to internal stress field.
   - By multiplying this stress field with Burgers vector we calculate The force (From Equation 2.32) experienced by the ith dislocation.By doing this process in a loop and adding the calculated force in previous value of force ,we calculate the total force applied by all other dislocations.
   - From equations 2.20 and 2.21, we can get the new coordinate position of dislocation firstly by forward difference, for further steps we will use central difference method for getting more accuracy in calculation.
   - These calculation are done for every dislocation and we get a new set of coordinates of dislocation.

3. These steps are iterated with very small time-step and we get the new positions of dislocations successively with further time steps.

These data in form of coordinates of dislocations is checked with data obtained analytically. We observed that the computational data is converging properly with analytical data when time-step is taken very less (in the order of$\sim$ 0.001).

2.8 Flow Chart for Time Integration Method

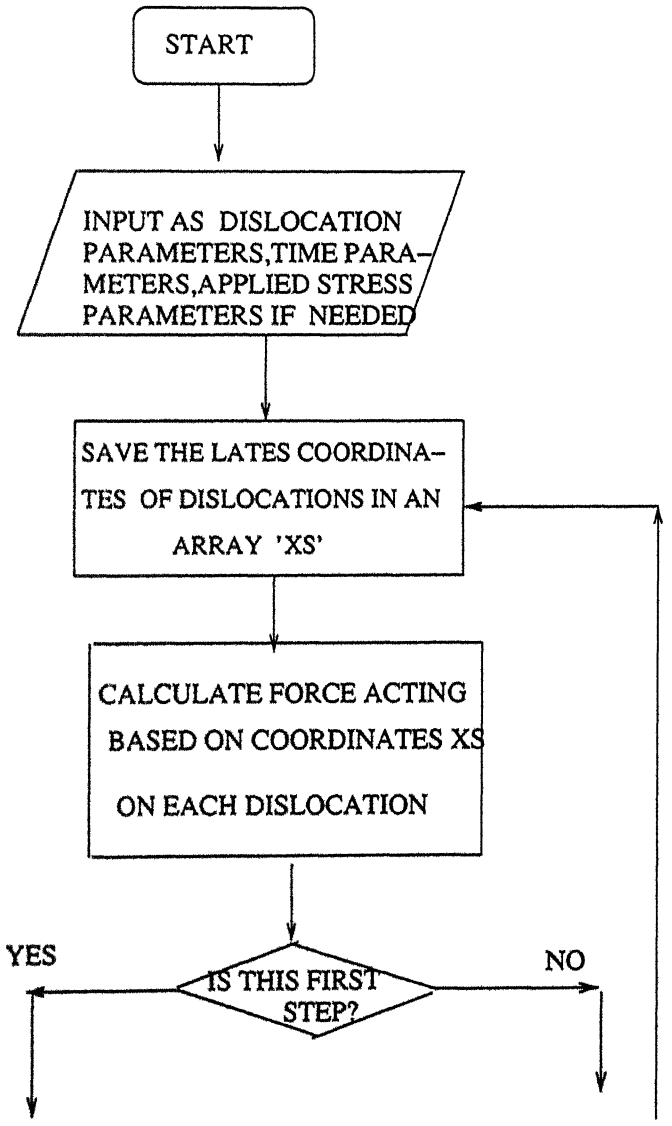

CONTINUE ON NEXT PAGE

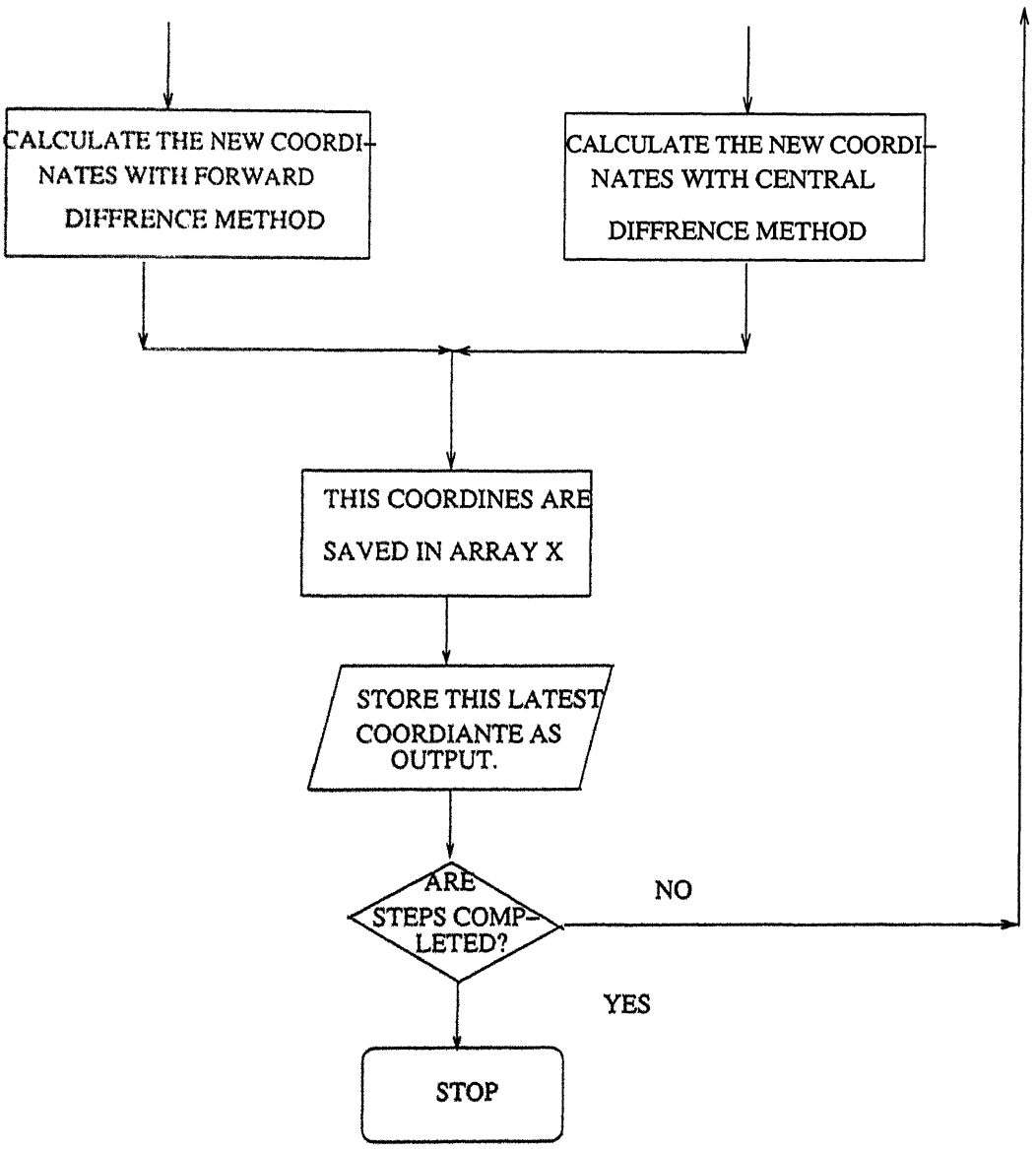

Figure 2.11: Computational Flow Chart

Chapter 3

One Dimensional Simulation

It should be noted that *in this thesis we are treating only unit pure edge dislocations*, however the dislocations are of both positive and negative type.

3.1 Case I:-Only with Internal Stress

For evaluating the behavior of two dislocations, we will put positive unit dislocation at x_0 distance while a negative unit dislocation is placed on the $-x_0$ distance from origin on x-axis,as shown in Fig.3.1.

3.1.1 Analytical Solution

Here only two dislocations are in a line for interacting with each other. The positive dislocation will be influenced by stress field of the negative dislocation and vice versa. The stress field of negative dislocation (from equation 2.27) will be

$$F_x = -\frac{1}{(x^+ - x^-)} \tag{3.1}$$

with *stress field keeping all constant terms unit.*
x^+ and x^- shows x coordinate of positive dislocation and negative dislocation respectively. On putting $x^+ = x$ and $x^- = -x$, above equation can be written.

$$\frac{\mathrm{d}x}{\mathrm{d}t} = -\frac{1}{2x} \tag{3.2}$$

On integrating:

$$\int \mathrm{d}x 2x = -\int \mathrm{d}t$$

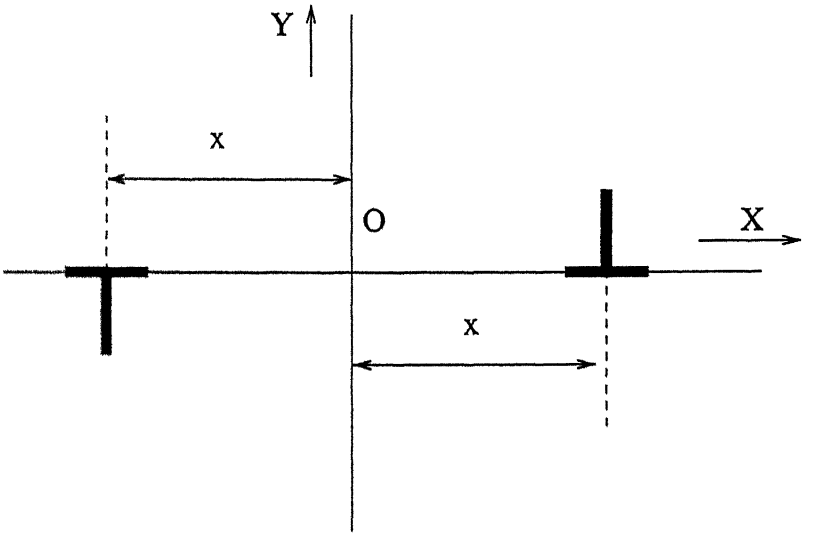

Figure 3.1: Two Dislocations in a line.

$$x^2 = -t + C \qquad \text{Where } C \text{ is integration constant} \tag{3.3}$$

Boundary condition for positive dislocation is:
For t=0 x=x_o
On applying this boundary condition to the equation 3.2 , we get the analytical solution in the following form.

$$x = \sqrt{x_0^2 - t} \tag{3.4}$$

We have taken $x_0 = 1$, so the analytical solution is:

$$x = \sqrt{1 - t} \tag{3.5}$$

3.1.2 Computational Solution

For iterating, the equation 3.2 can be written from difference scheme as following:

$$\frac{x_{i+1} - x_{i-1}}{\Delta t} = \frac{1}{2x_i}$$

$$x_{i+1} = x_{i-1} + \Delta t \frac{1}{2x_i} \tag{3.6}$$

The Error in analytical and computational result is

$$\text{Error} = x_{i+1} - \sqrt{x_0^2 - t} \tag{3.7}$$

x_{i+1} is the position of positive dislocation at time t
Further, we will see that the computational results are converging with analytical results.

3.2 Case II:-Internal Stress and Externally Applied Stress

We will simply add the applied stress to the internal stress of dislocations. We are applying a sinusoidal stress, which varies as shown in Fig.3.2.

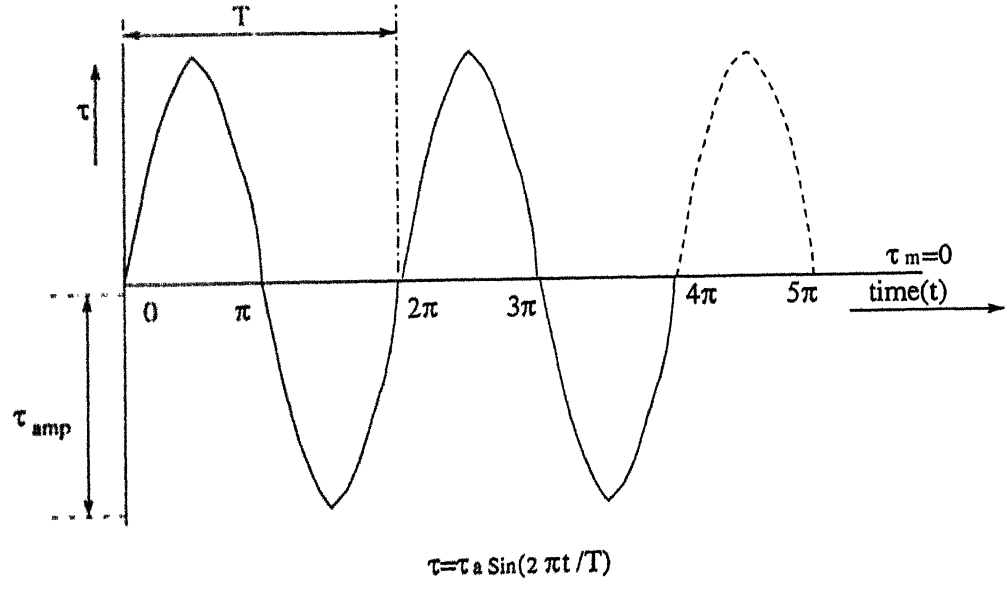

Figure 3.2: External Shear Stress.

The external stress can be written as,

$$\tau_{ext} = \tau_m + \tau_a \sin \frac{2\pi t}{T}$$

Where τ_m, τ_a and T are mean,amplitude and periodicity of the external shear stress.

3.2.1 Analytical Result

Considering only external stress

$$\frac{\mathrm{d}x(t)}{\mathrm{d}t} = \tau_{ext}$$

On integrating,

$$x(t) = C + \tau_m t + \frac{T\tau_a}{2\pi}\left(1 - \cos\frac{2\pi t}{T}\right)$$

Where C is the integration constant.
Boundary condition: $t = 0, x(t) = x_0$

$$x(t) = x_0 + \tau_m t + \frac{T\tau_a}{2\pi}\left(1 - \cos\frac{2\pi t}{T}\right) \tag{3.8}$$

Including the *internal stress*, The total force will be:

$$\frac{\mathrm{d}x^i(t)}{\mathrm{d}t} = -\frac{1}{(x^i - x^j)} + b_i\left(\tau_m + \tau_a \sin\frac{2\pi t}{T}\right) \tag{3.9}$$

For positive dislocation's coordinate we can write above equation as,

$$\frac{\mathrm{d}x^+}{\mathrm{d}t} = -\frac{1}{(x^+ - x^-)} + \left(\tau_m + \tau_a \sin\frac{2\pi t}{T}\right) \tag{3.10}$$

For negative dislocation,

$$\frac{\mathrm{d}x^-}{\mathrm{d}t} = -\frac{1}{(x^- - x^+)} - \left(\tau_m + \tau_a \sin\frac{2\pi t}{T}\right) \tag{3.11}$$

By adding and subtracting equations 3.10 and 3.11 and putting:

$$\frac{x^+ + x^-}{2} = \eta \qquad \text{and} \qquad \frac{x^+ - x^-}{2} = \xi$$

We get two equations in terms of ξ and η,

$$2\frac{\mathrm{d}\xi}{\mathrm{d}t} = -\frac{1}{\xi} + 2\tau_{ext} \tag{3.12}$$

$$2\frac{\mathrm{d}\eta}{\mathrm{d}t} = 0 \tag{3.13}$$

Boundary conditions: when t=0, $\xi = x_0$ and $\eta = 0$

The equation 3.12 can be written as,

$$\frac{d\xi}{dt} = -\frac{1}{2\xi} + \tau_{ext} \tag{3.14}$$

Above equation is a non-linear differential equation ,so we will use following iteration procedure for numerical solution.

$$\frac{\xi_{i+1} - \xi_{i-1}}{2\Delta t} = -\frac{1}{2\xi_i} + \tau_a \sin\frac{2\pi\Delta t}{T}$$

When τ_m is taken 0.

$$\xi_{i+1} = \xi_{i-1} + 2\Delta t\left(-\frac{1}{2\xi_i} + \tau_a \sin\frac{2\pi\Delta t}{T}\right) \tag{3.15}$$

From above equation we can get successive values of ξ, which is equal x-coordinate of positive dislocation.

3.2.2 Computational Result

The equation for computational result:

$$\frac{x_{i+1} - x_{i-1}}{2\Delta t} = b_i\left(-\frac{1}{2x_i} + \tau_m + \tau_a \sin\frac{2\pi t}{T}\right)$$

keeping $\tau_m = 0$

$$x_{i+1} = x_{i-1} + 2\Delta t b_i\left(-\frac{1}{2x_i} + \tau_a \sin\frac{2\pi t}{T}\right) \tag{3.16}$$

Now we can get the plots with different set of values of τ_a and T for two dislocations. The graphs of externally applied stress condition for two dislocations are depicted in chapter-5.

3.2.3 For many dislocations

The dislocations of both positive and negative signs are arranged on x-axis as shown in Fig.3.3. Dislocations will interact with all other dislocations by the force in x-direction only. In Internal stress case, The effective force between them will be only due to resultant τ_{xy} of all dislocations.
The effective formula for many dislocations simulation is

$$x_{i+1} = x_{i-1} + 2\Delta t b_i \sum_{i=1}^{j} \tau_{xy}(i,j) \tag{3.17}$$

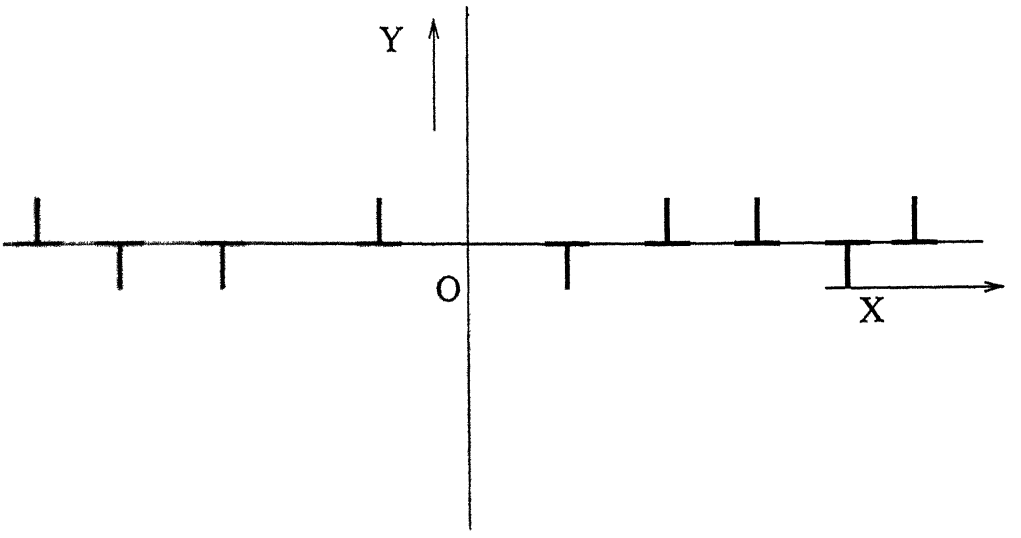

Figure 3.3: Dislocations on x-axis.

When $j \neq i$

Chapter 4

Two Dimensional Simulation

4.1 Internal Stress

4.1.1 Dislocation Patterning

Firstly we will discuss about the behavior of dislocations due to internal stress field only. The dislocations are arranged in two-dimensional field randomly as shown in Fig. 4.1.

We are going to neglect the inter-slip motion,so we will neglect the force acting in y direction. The effective stress field will be only τ_{xy}. The dislocations will glide only in their slip planes.

The force acting on any ith dislocation can be calculated from equations (2.31) and (2.32).

$$\frac{\mathrm{d}x}{\mathrm{d}t} = b_i\left(\sum_{i=1}^{j} b_x(j)\sigma 1_{xy} + b_y(j)\sigma 2_{xy}\right) \tag{4.1}$$

Where $j \neq i$

Where b_x and b_y are Burgers vector's components of jth dislocation.$\sigma 1_{xy}$ and $\sigma 2_{xy}$ are stress field because of b_x and b_y of jth dislocation in position of ith dislocation. The expression for $\sigma 1_{xy}$ and $\sigma 2_{xy}$ can be got from equations (2.28) and (2.30).

By differential scheme we can get the successive coordinates of dislocations in further time steps. By iterating the above procedure for time of integration, we get the data as the coordinates of all dislocations with different time steps.

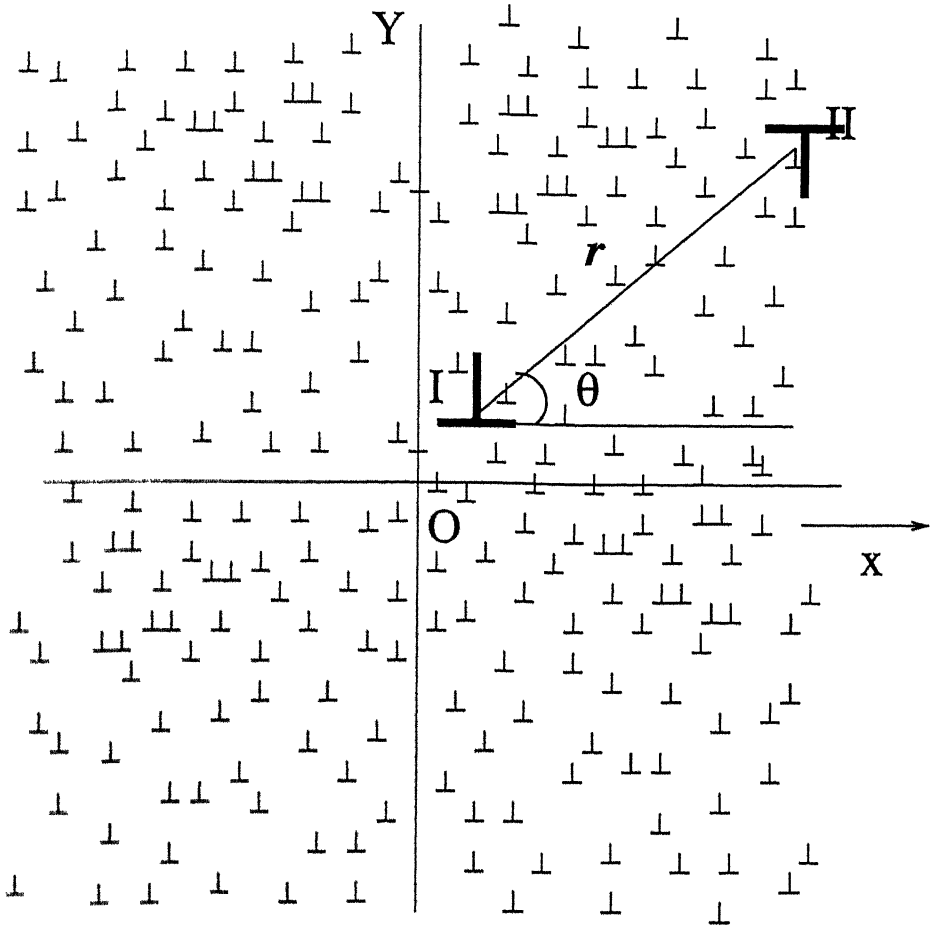

Figure 4.1: Dislocations in two dimensional-field.

The plot of dislocation-patterning with internal stress are given in chapter-5

4.1.2 Dynamics of Dislocation Wall

Later we will see that due to internal stress the dislocations form the walls of dislocations (vertical dislocation-patterning). Dislocation-wall move with time away from each other. The velocity of these both walls can be calculated by the following steps.

1. Firstly we divided the whole area (on which dislocations are moving) in

many small n vertical strips. That can be written in mathematical form as:

$$\Delta x = \frac{x_{max} - x_{min}}{n}$$

2. Now we can count the no. of positive and negative dislocations in each Δx region. The region on which no. of dislocations is highest contains the dislocation wall.

3. In different time step we can get the position of dislocation by step 2. So we can get the plot between x-position and time for walls of positive dislocations and negative dislocations. So we can estimate the velocity of dislocation walls.

4.2 Internal and External Stress

For including the external stress we have to add the external stress term in the equation 2.31, equation will turn out to be.

$$\frac{dx}{dt} = b_i\left(\sum_{i=1}^{j}\tau_{xy}(i,j) + \tau_{ext}\right) \tag{4.2}$$

In terms of parameters of cyclic external stress like mean, amplitude and periodicity of the stress the above equation can be written as.

$$\frac{dx}{dt} = b_i\left[\sum_{i=1}^{j}\tau_{xy}(i,j) + \left(\tau_m + \tau_a \sin\frac{2\pi t}{T}\right)\right] \tag{4.3}$$

Rest procedure is same as internal stress computational procedure.

4.3 Computational Flow Chart

Computational flow chart for velocity of dislocation-wall is drawn on the next page as Fig.4.2.

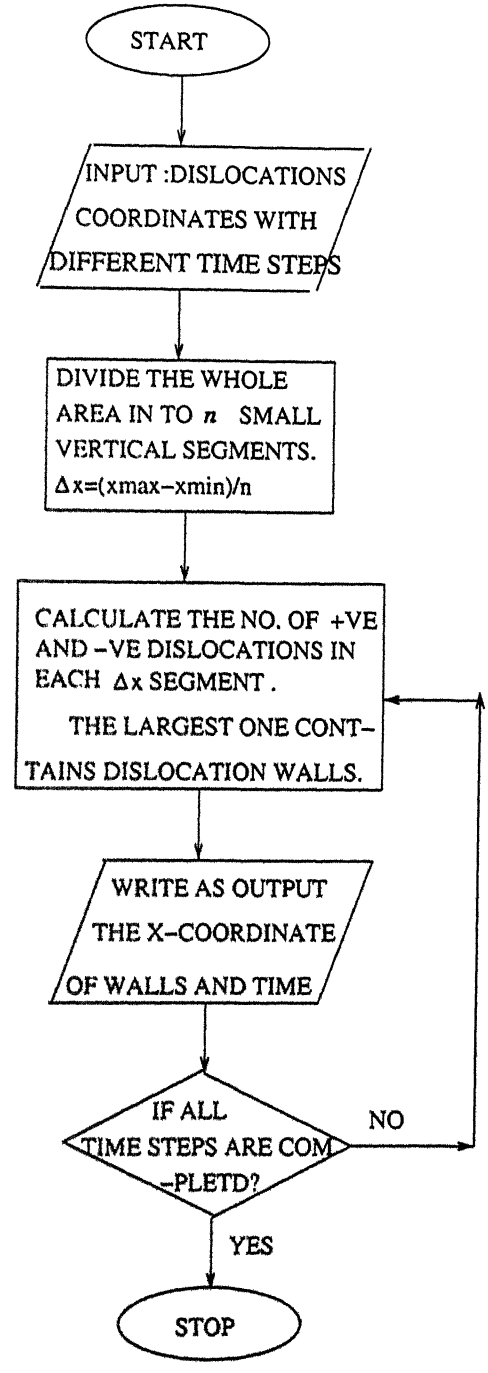

Figure 4.2: Flow Chart For Velocity of Dislocation-Wall

Chapter 5

Results and Discussion

The dislocations are studied for their movement in their slip planes in influence of two types of stress fields as described earlier.

1. Only by internal stresses.
2. By internal as well as external stresses.

We will see further the results for one-dimensional and two-dimensional array of dislocations.

5.1 Simulation for Two Dislocations

5.1.1 Only Internal Stress

The dislocations are placed on x-axis.Dislocation-I will interact with other by stress field of dislocation-II and vice-versa. The result is shown in Fig. 5.1.The figure is showing computational as well as analytical results, which are overlapping.
EXPLAINATION:

1. The dislocations are gliding towards each-other with time before annihilating.
2. The time taken for annihilation depends on their initial positions.

5.1.2 Internal Stress and External Stress

We want to know the behavior of dislocation-gliding in presence of external stresses. We will see the effect in gliding with different amplitude and periodicity of external stress.The mean stress is kept 0 in all results. These results are depicted from Fig. 5.2a to 5.2f

EXPLAINATION:

1. The dislocations gliding is unaffected by very small value of cyclic stress. (Fig. 5.2a)
2. When we increase the amplitude of external stresses, It starts to affect the dislocation motion.The stress tends to drive the dislocation gliding. (Fig 5.2b)
3. When the external stress is very high.The dislocation prominently drives the dislocation motion.(Fig. 5.2d and 5.2f)

5.2 Many Dislocations in a line

When many dislocations that randomly distributed in a line are subjected to internal stress meet of the dislocations remain around their initial coordinates.

EXPLAINATION:

1. the dislocations glide only in x-axis.
2. One negative dislocation moves to $+\infty$ while one negative dislocation to $-\infty$.(From Fig. 5.3a to 5.3c)
3. Most of dislocations vibrate around their original coordinates.

5.3 Two Dimensional Dislocation

5.3.1 With Internal Stress Only

EXPLAINATION:

1. the dislocations are moving in their glide planes only.
2. The dislocations are making mainly a two vertical clusters (walls) of positive dislocations and negative dislocations. Fig. 5.4c
3. The dislocation walls are moving to opposite direction with time.
4. From plot 5.6a we see that the velocity is decreasing firstly and later it is achieving approximate constant value.
5. velocity of positive and negative dislocation-walls are showing similarity.(Fig. 5.6b)
6. When *xmin* is increased successively the straight vertical wall (pattern) get defused. This is clear from Fig. 5.4c, 5.7a and 5.7b, in which plots only *xmin* is increasing
7. If there is intrinsic length scale then we see that the walls splitting into the form of a sin wave.If we increase the size of the intrinsic length scale successively, the wavelengh of the wave decreases (from Fig. 5.8a and 5.8b).

5.3.2 With Both Internal- and External-Stress Field

The related plots are from Fig. 5.9a to 5.9b.
EXPLAINATION:

1. In case of both stress fields the dislocations are getting their vertical pattern but with time they are being drived by external stress field .
2. Dislocation-walls are unstable with time .

5.4 Important Graphs and Plots

The graphs and plots are on next pages:

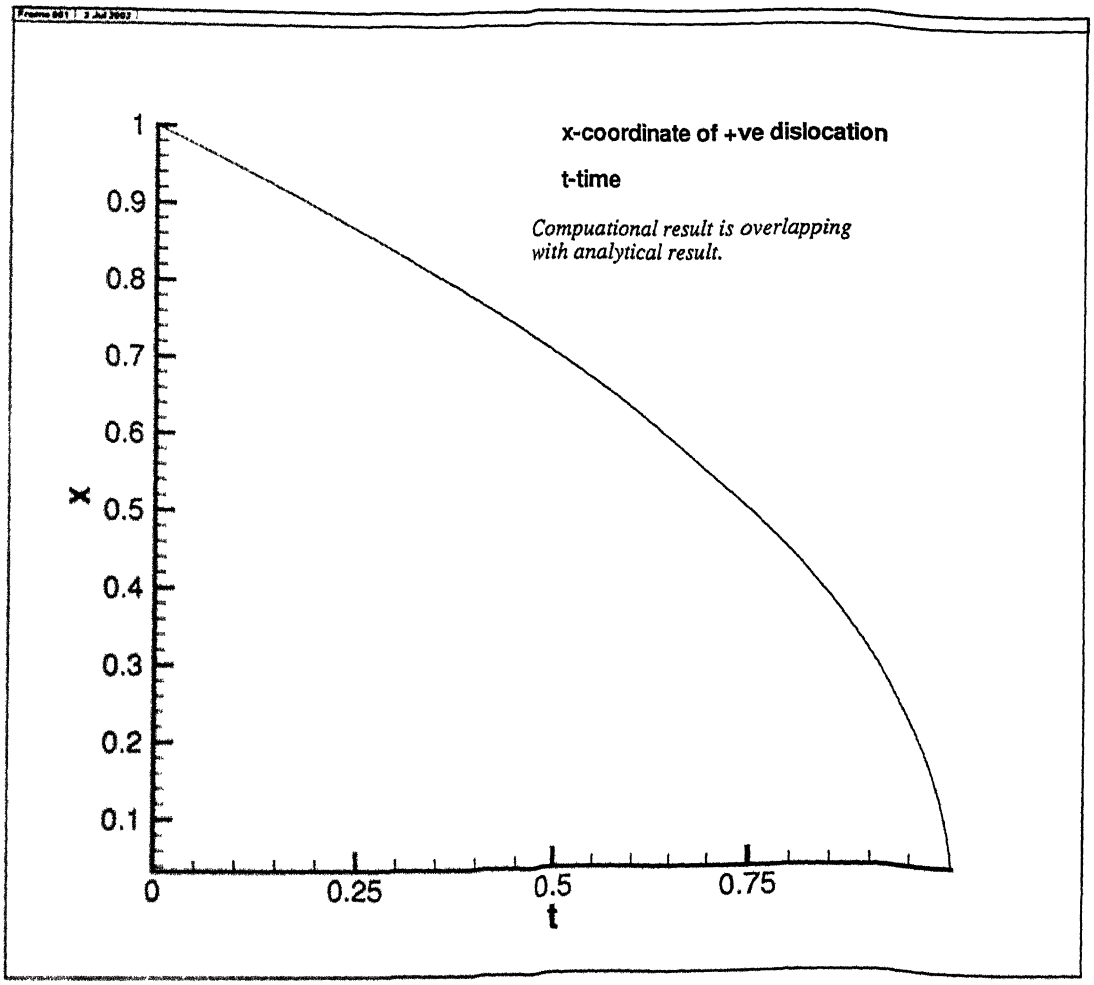

Figure 5.1: Positive dislocation's gliding with time by internal stress only

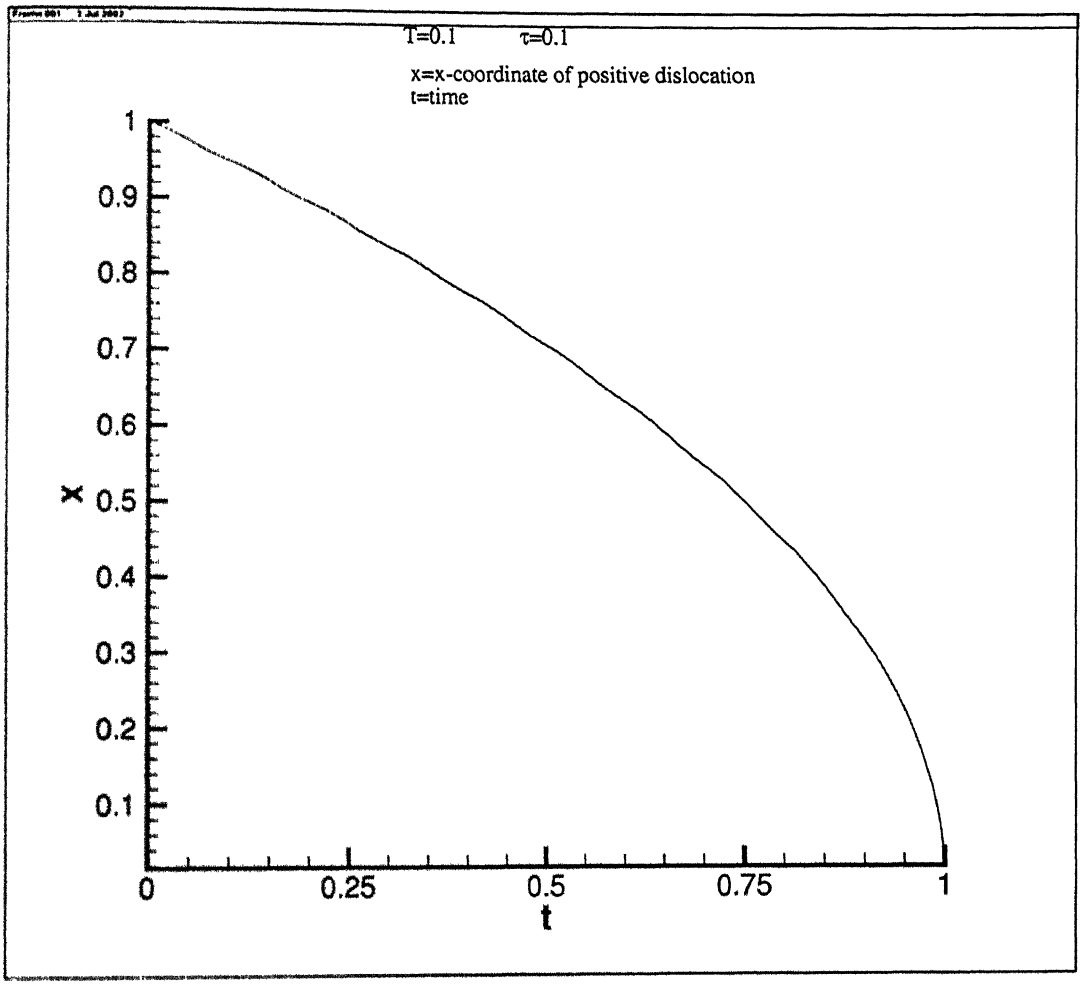

Figure 5.2a: Positive dislocation's gliding with external stress

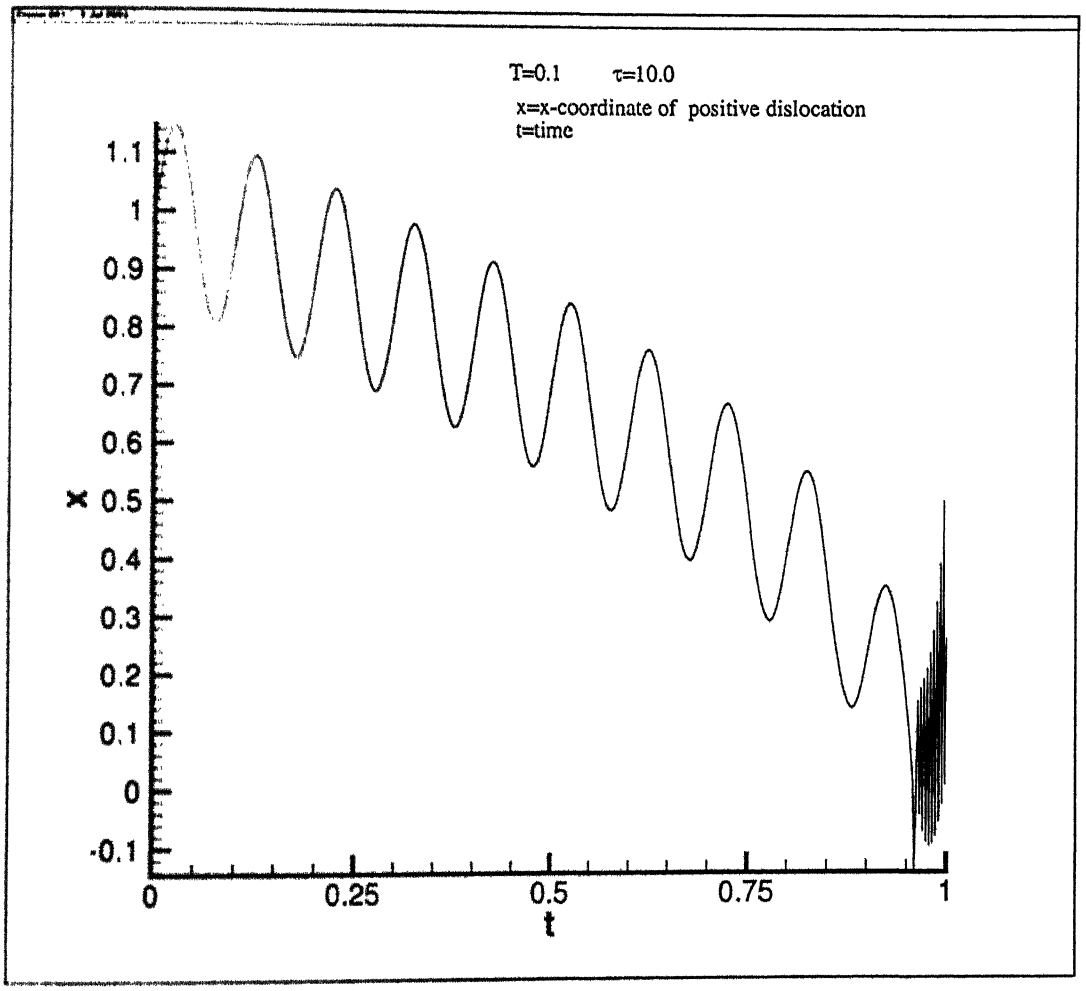

Figure 5.2b: Positive dislocation's gliding with external stress

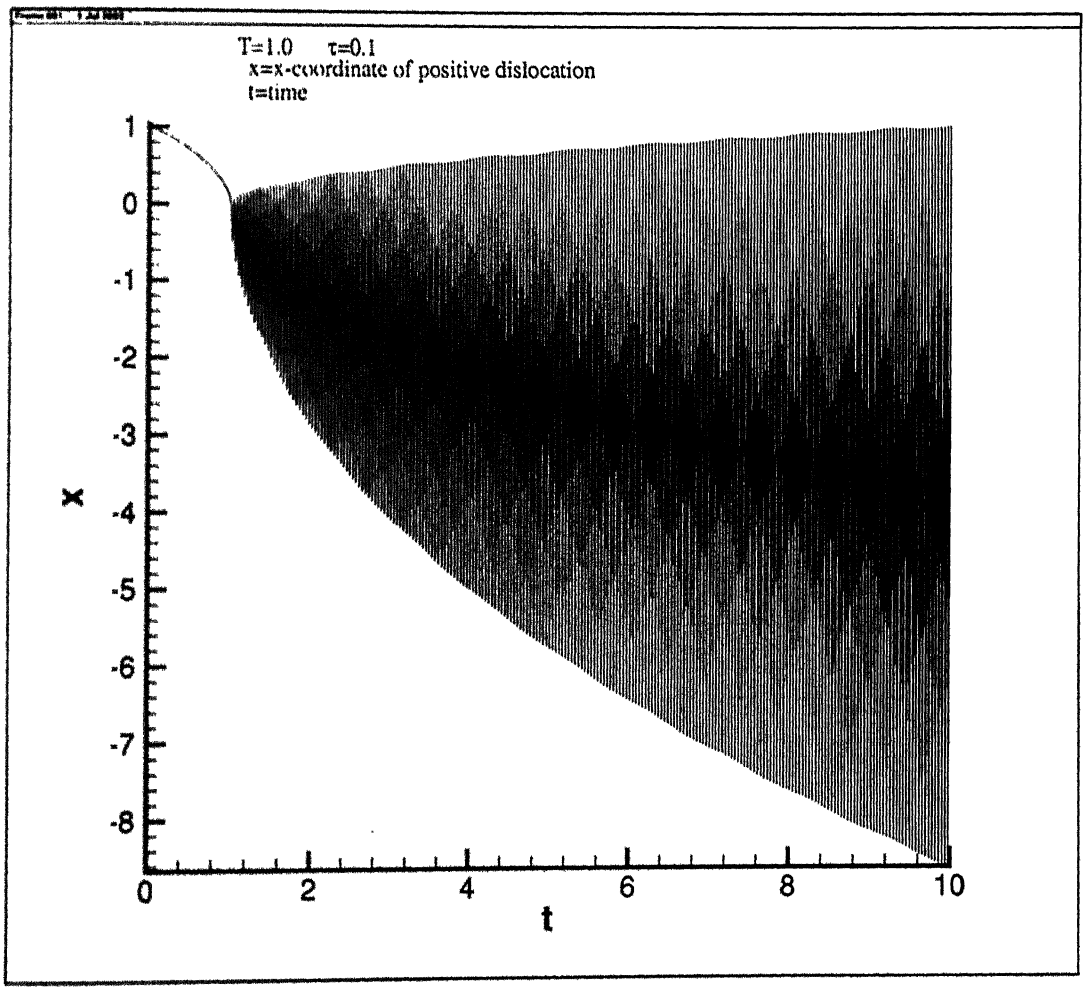

Figure 5.2c: Positive dislocation's gliding with external stress

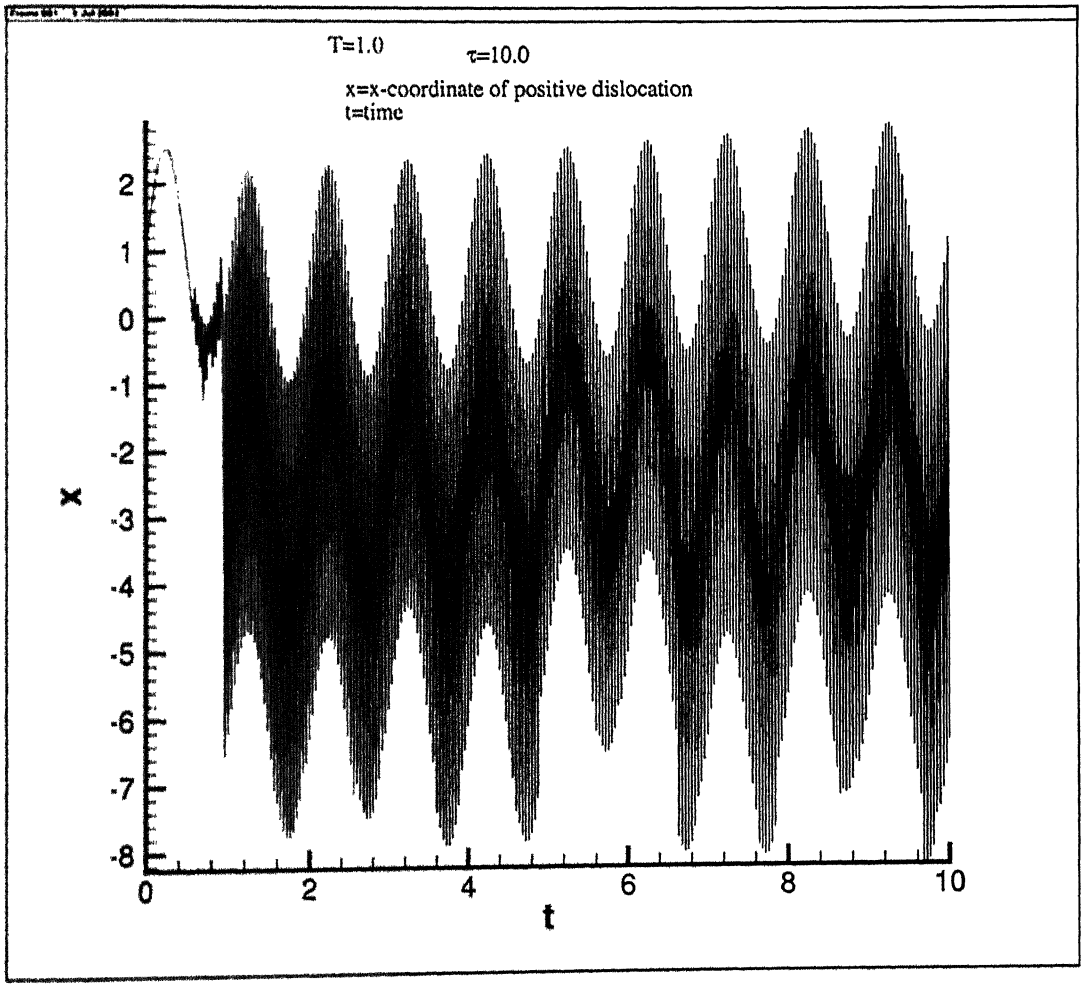

Figure 5.2d: Positive dislocation's gliding with external stress

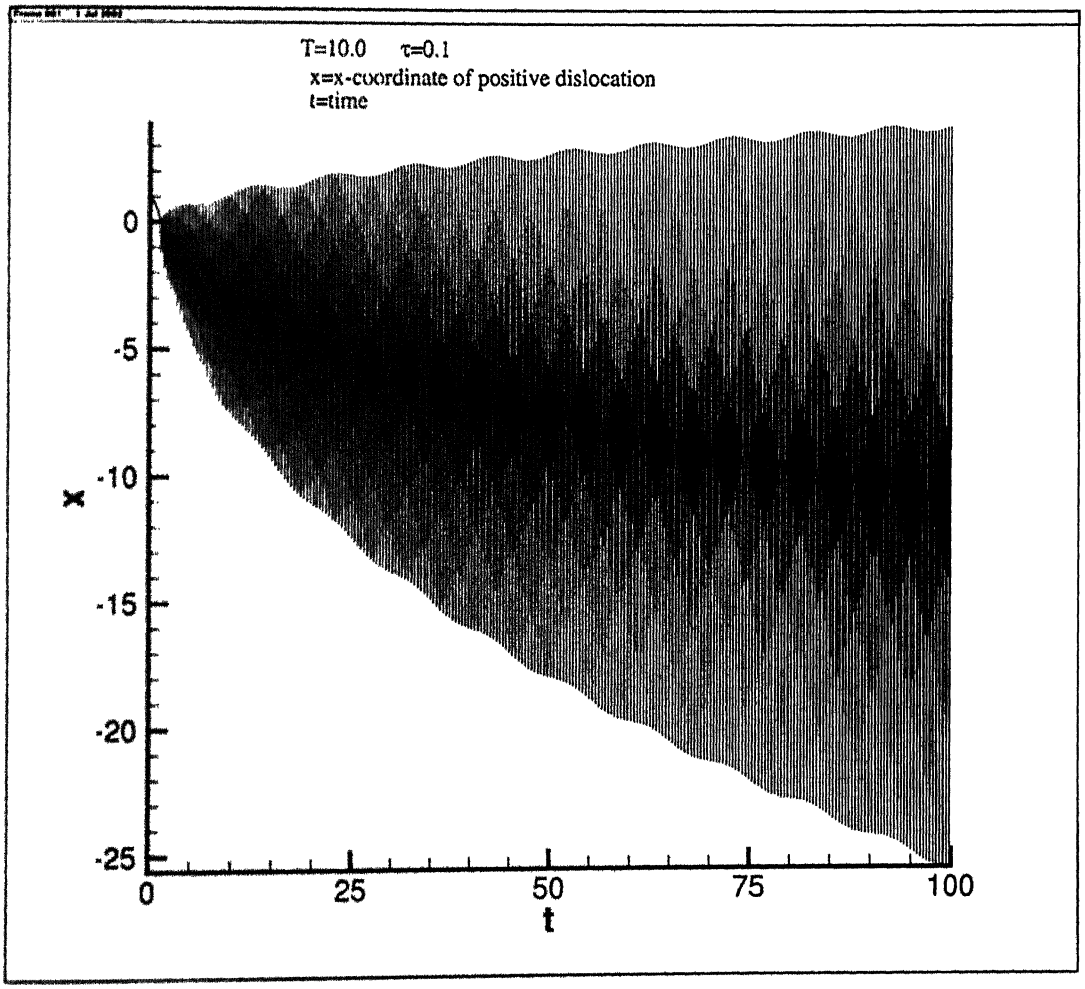

Figure 5.2e: Positive dislocation's gliding with external stress

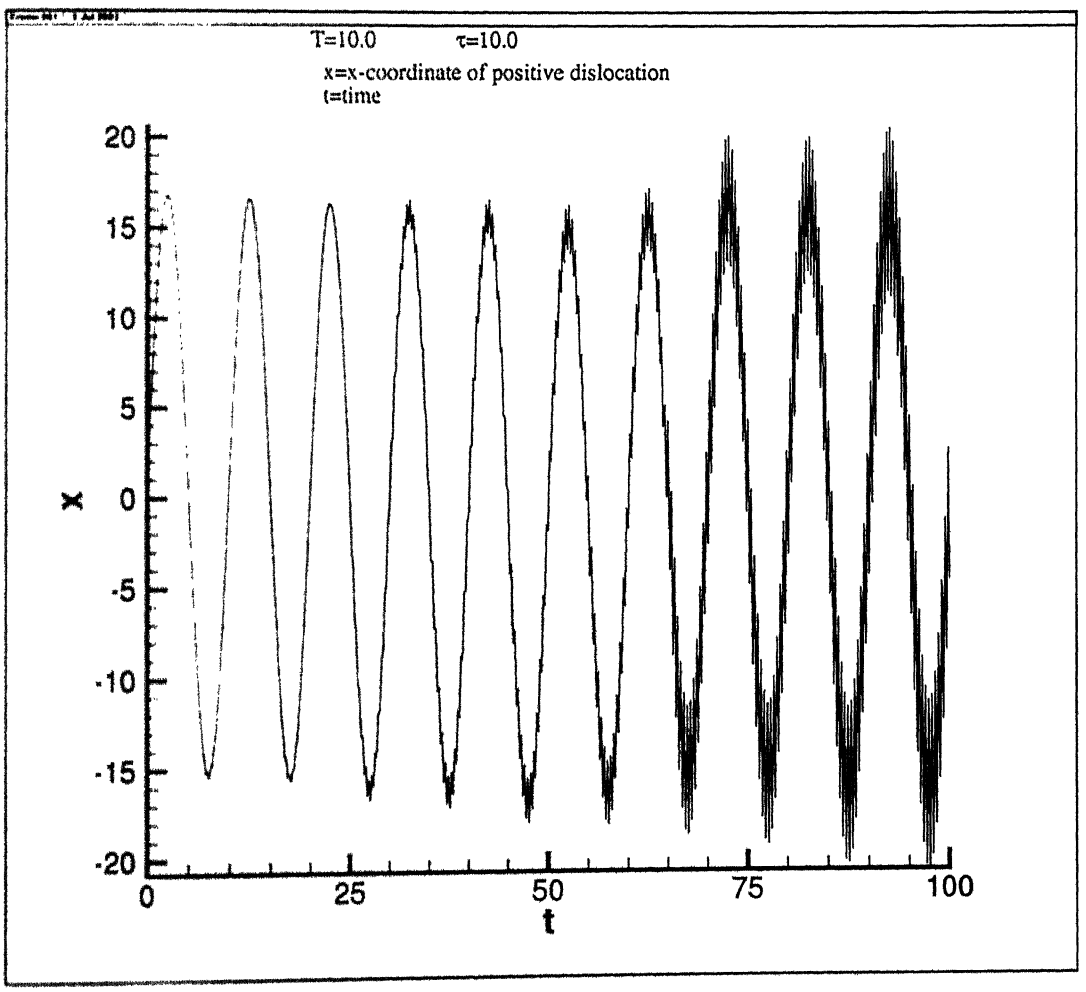

Figure 5.2f: Positive dislocation's gliding with external stress

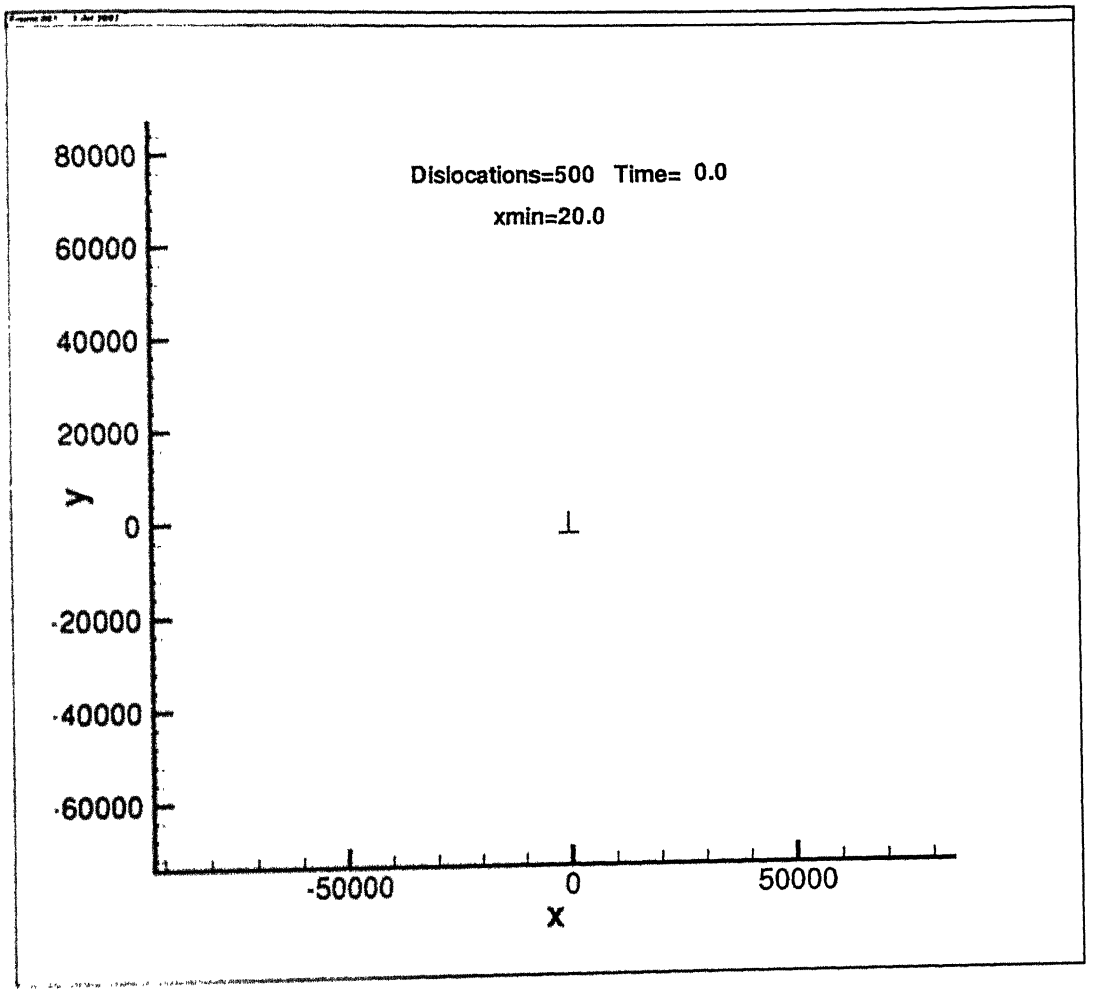

Figure 5.3a: Many dislocations on x-axis under internal stress only

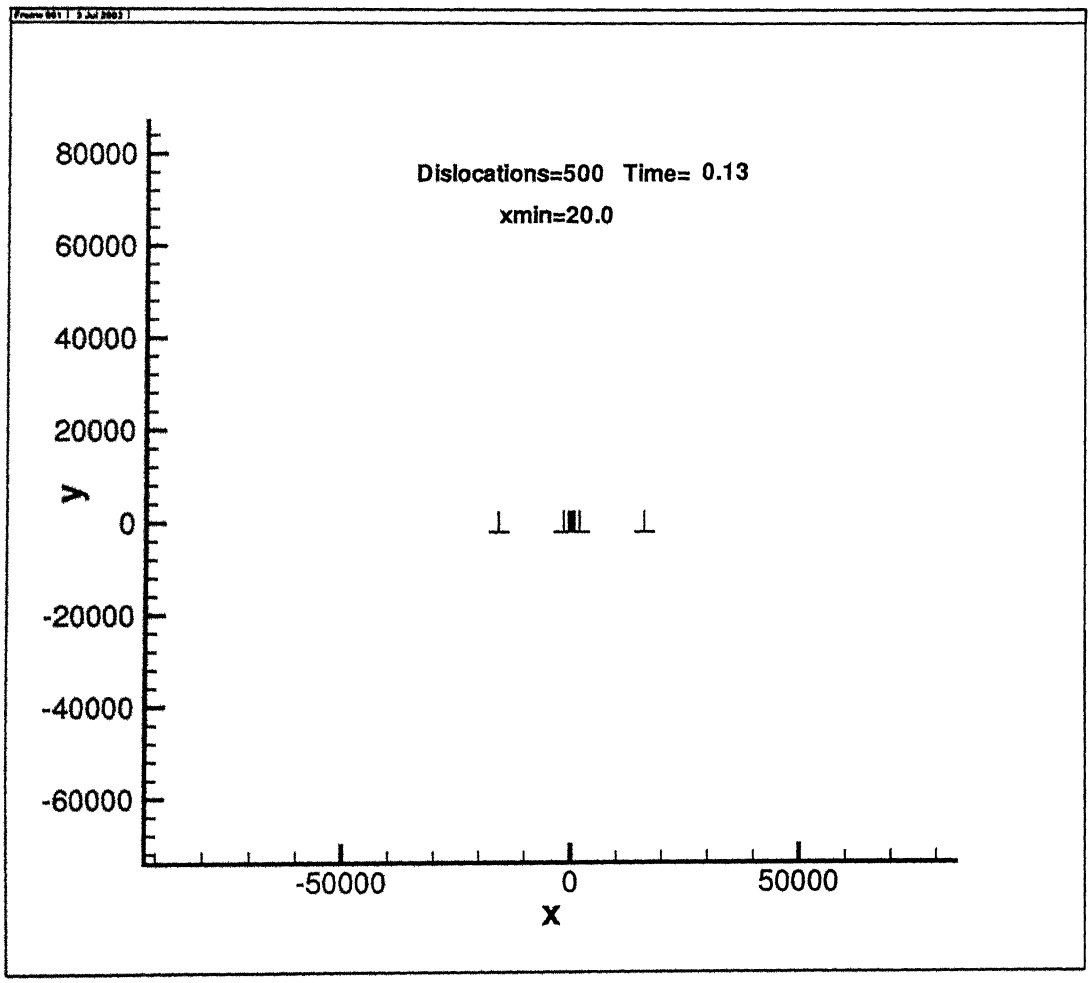

Figure 5.3b: Many dislocations on x-axis under internal stress only

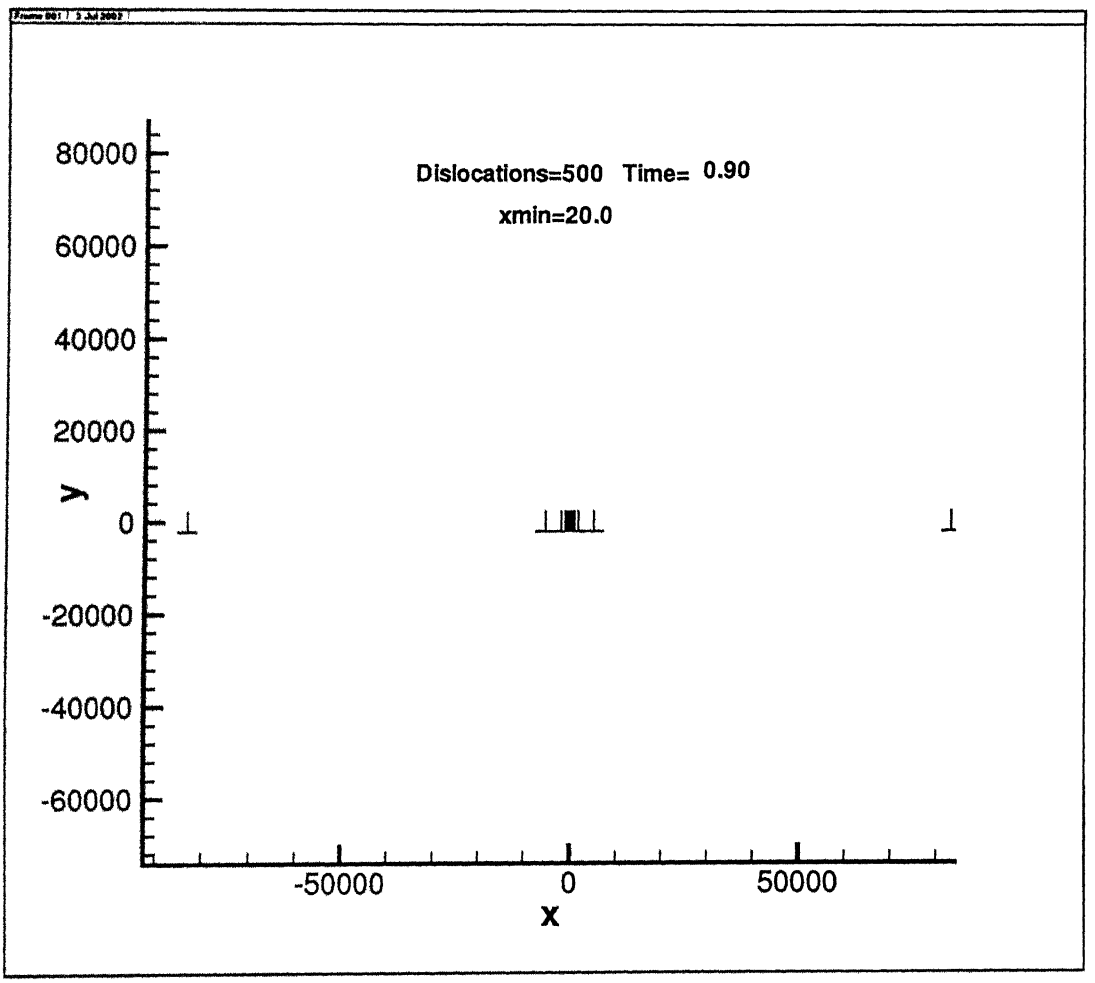

Figure 5.3c: Many dislocations on x-axis under internal stress only

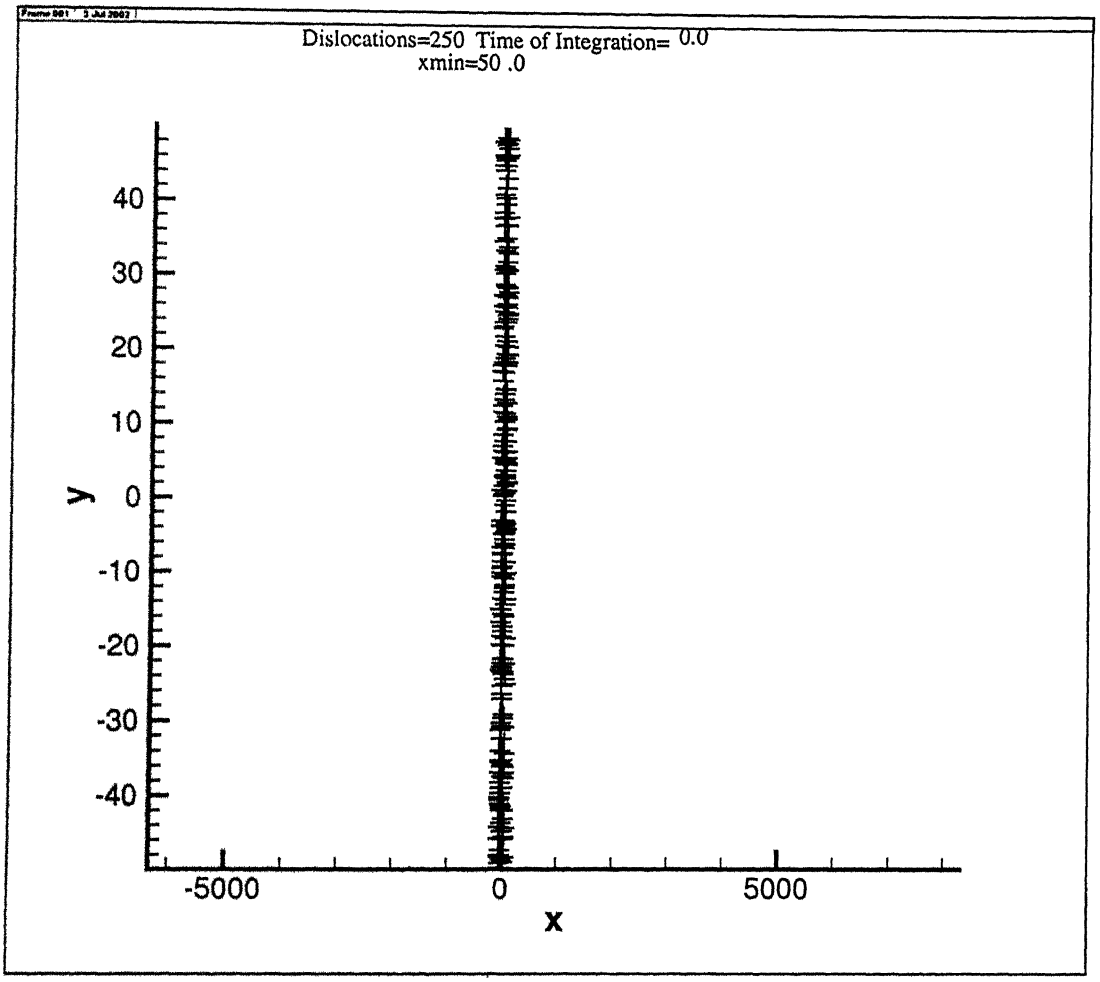

Figure 5.4a: 250 dislocations clustering with time

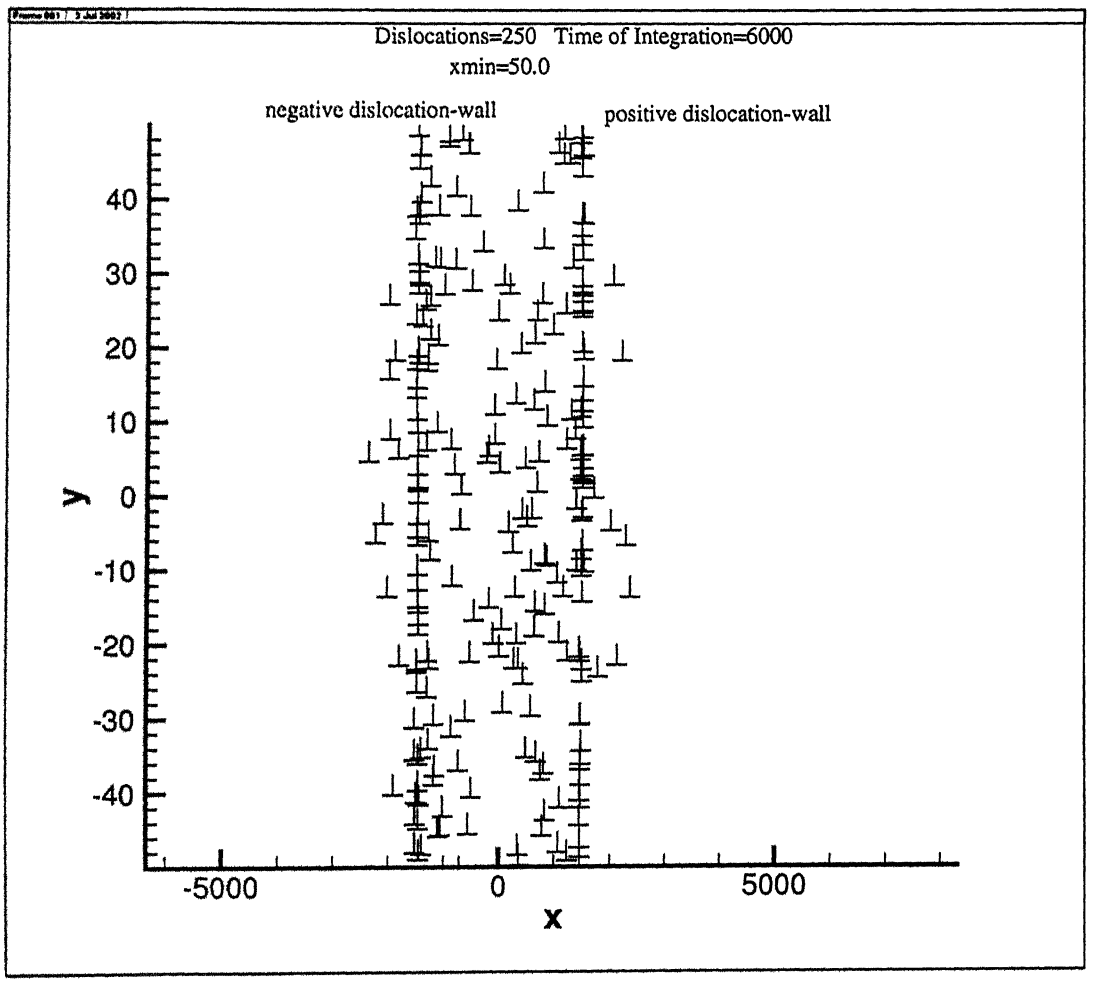

Figure 5.4b: 250 dislocations clustering with time

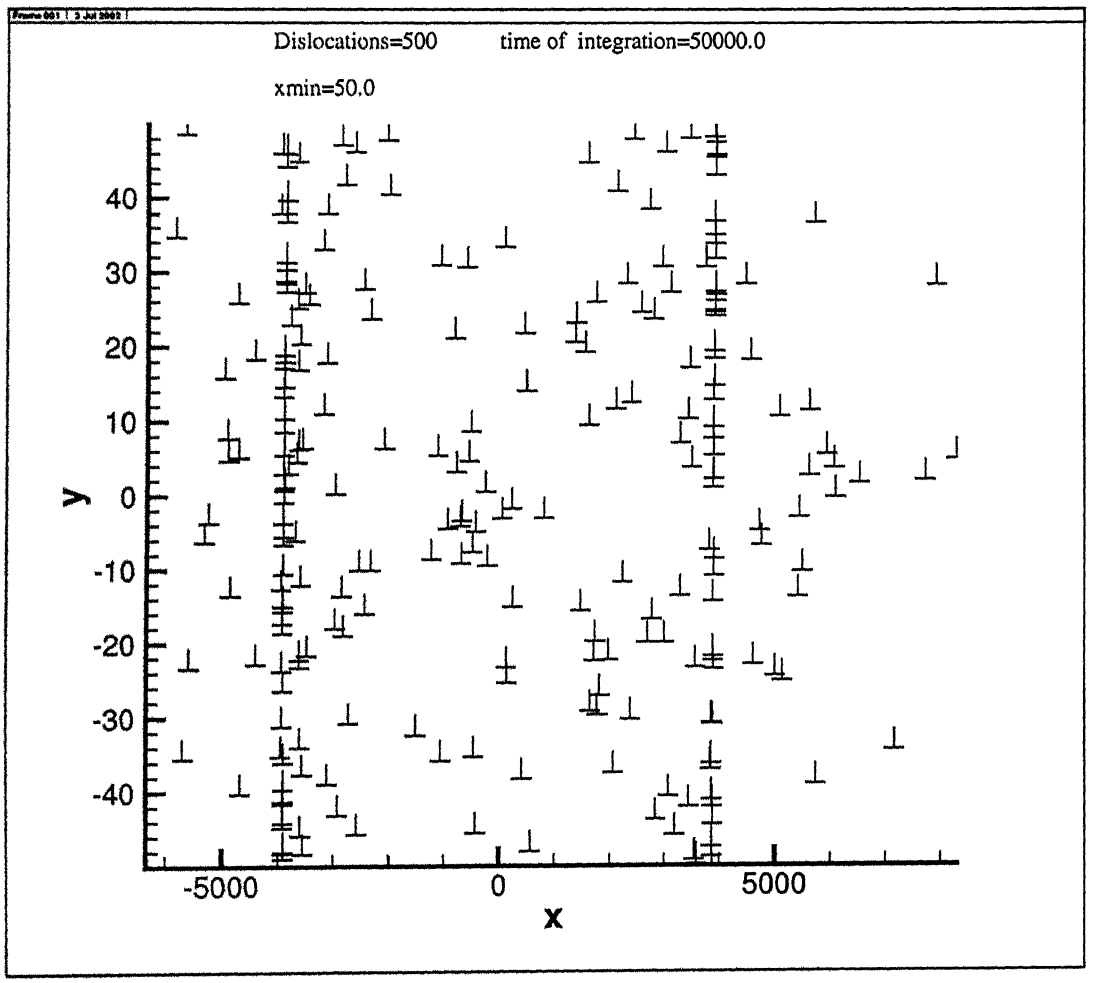

Figure 5.4c: 250 dislocations clustering with time

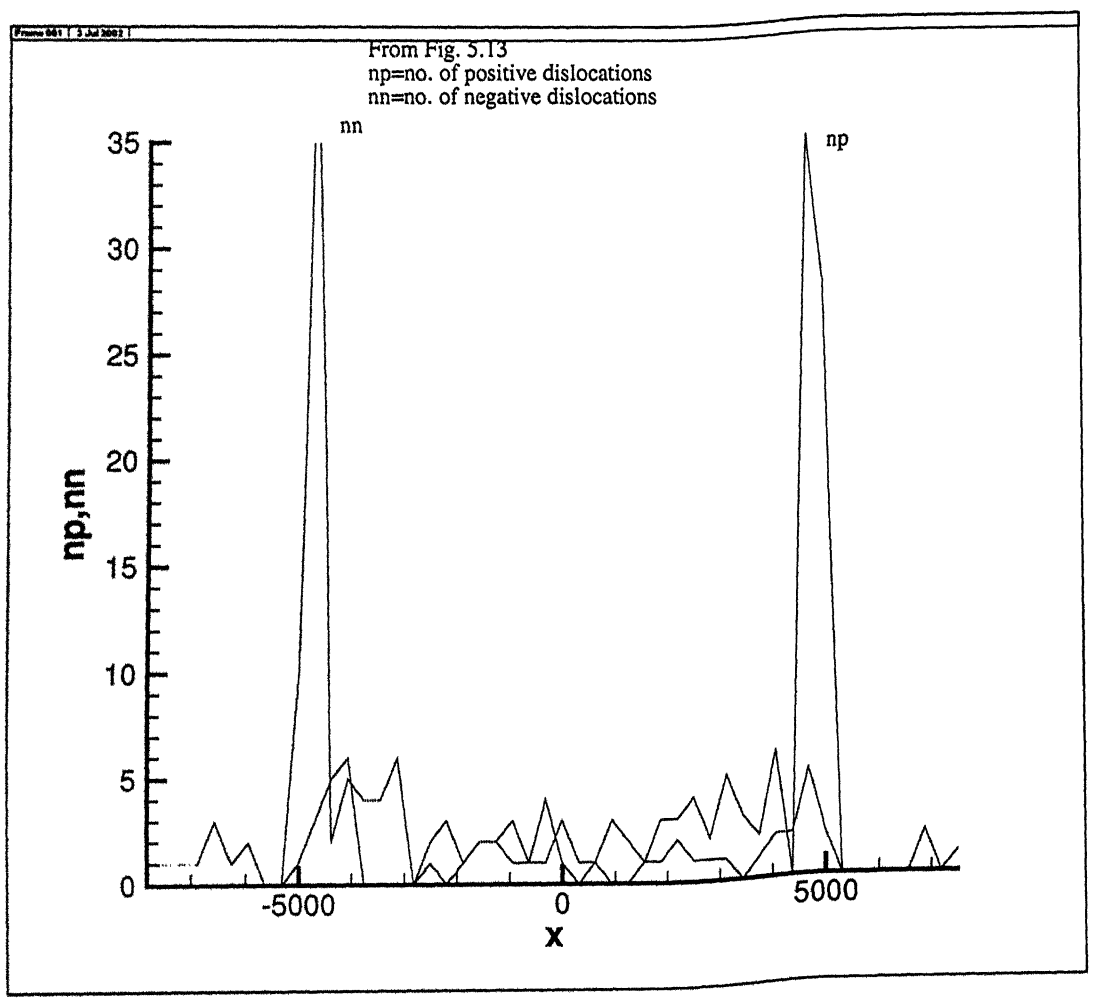

Figure 5.5: Density of 250 Dislocations After Integration

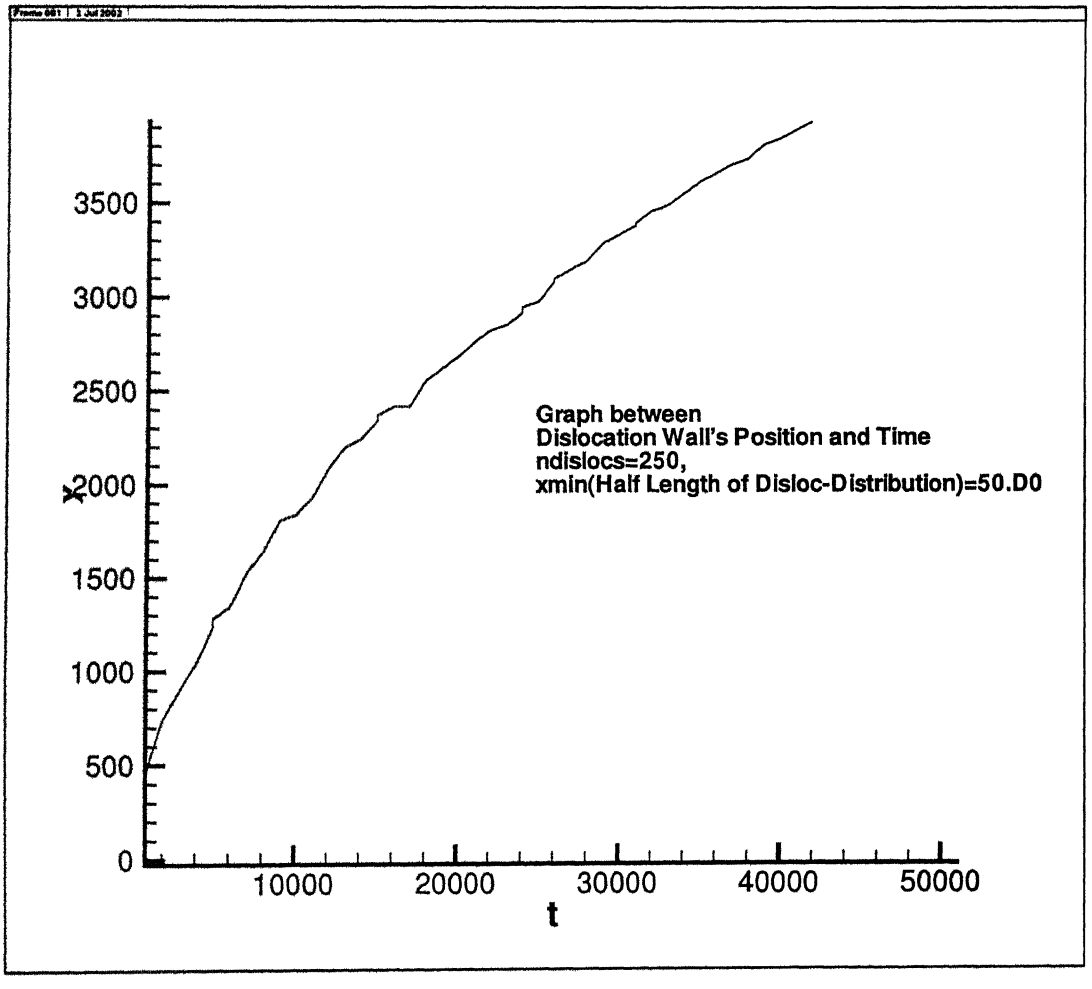

Figure 5.6a: Velocity of positive Dislocation Wall with 250 Dislocations

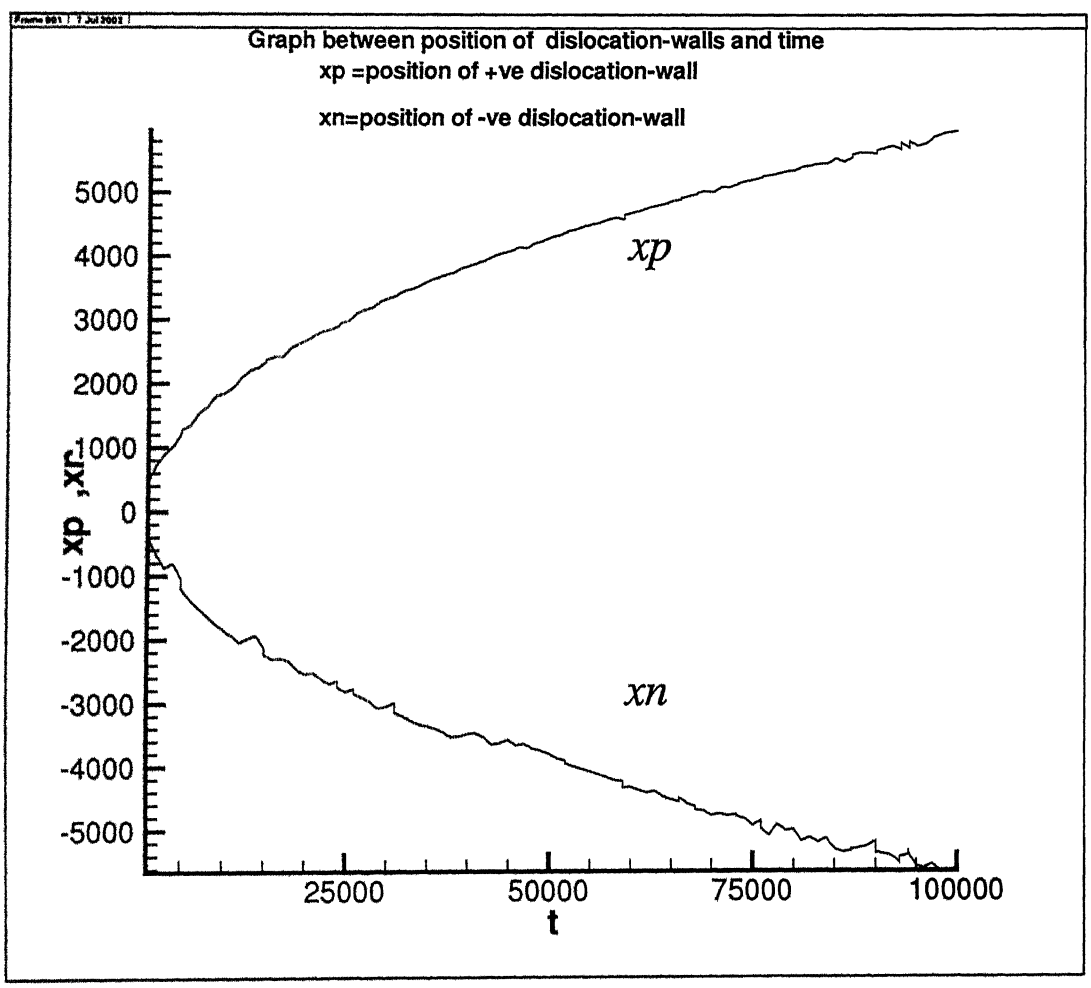

Figure 5.6b: Velocity of Both Walls

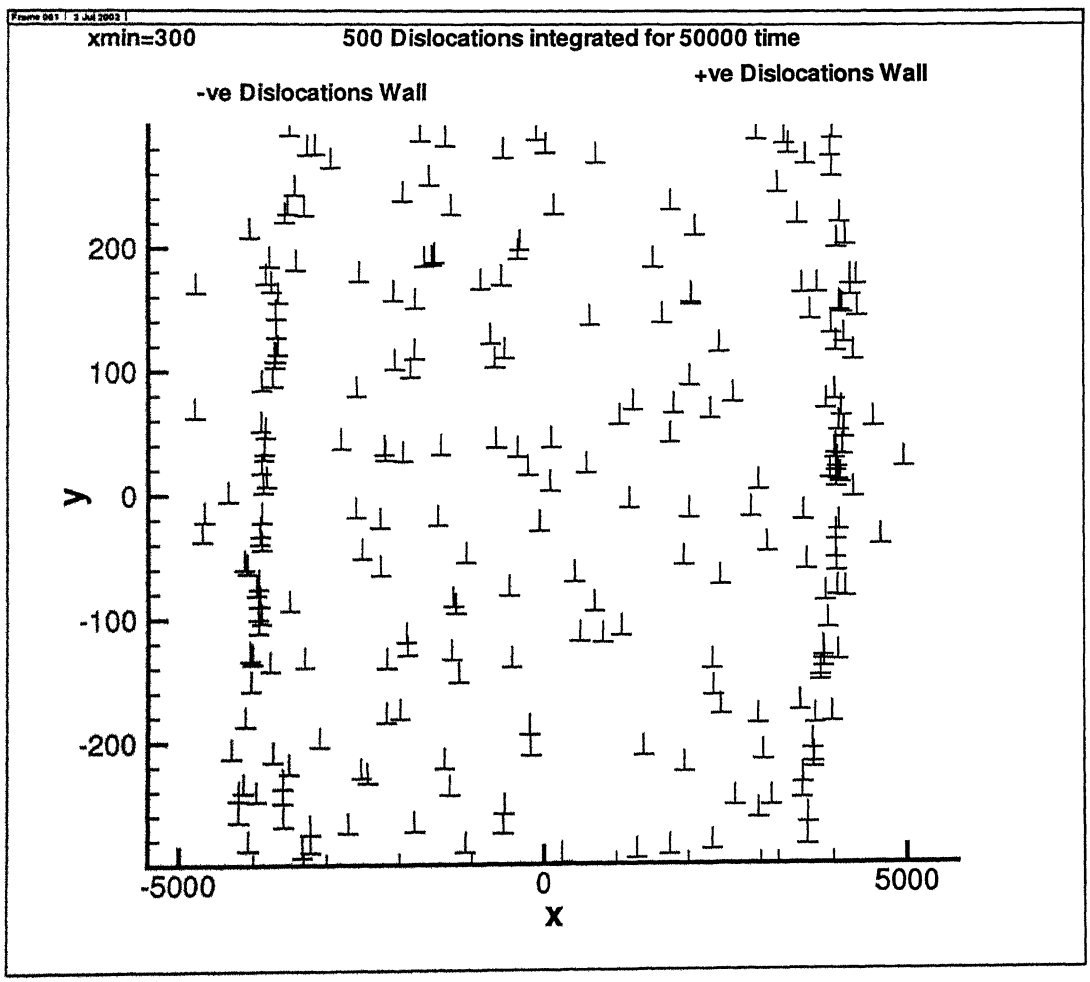

Figure 5.7a: Many Dislocations clustering with time: with different *xmin*

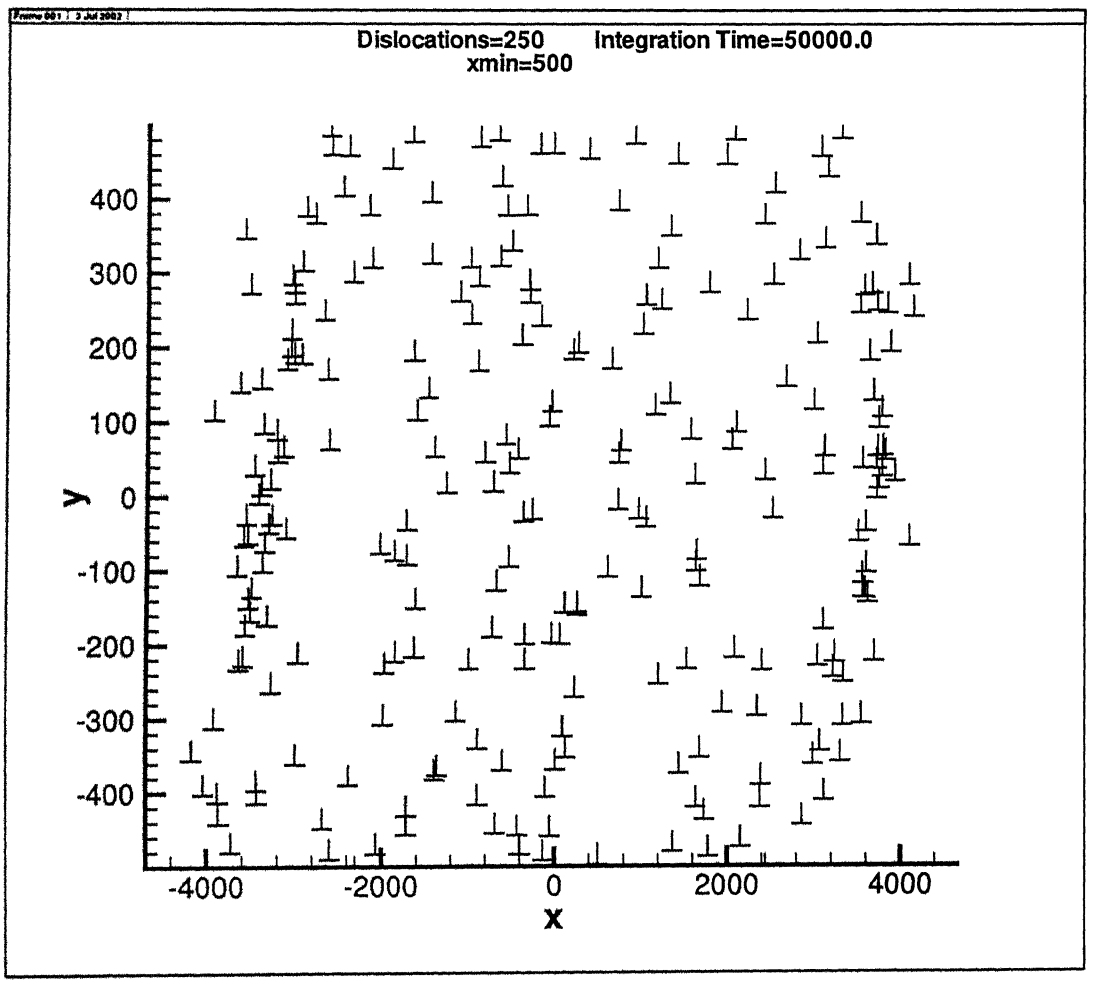

Figure 5.7b: Many Dislocations clustering with time: with different *xmin*

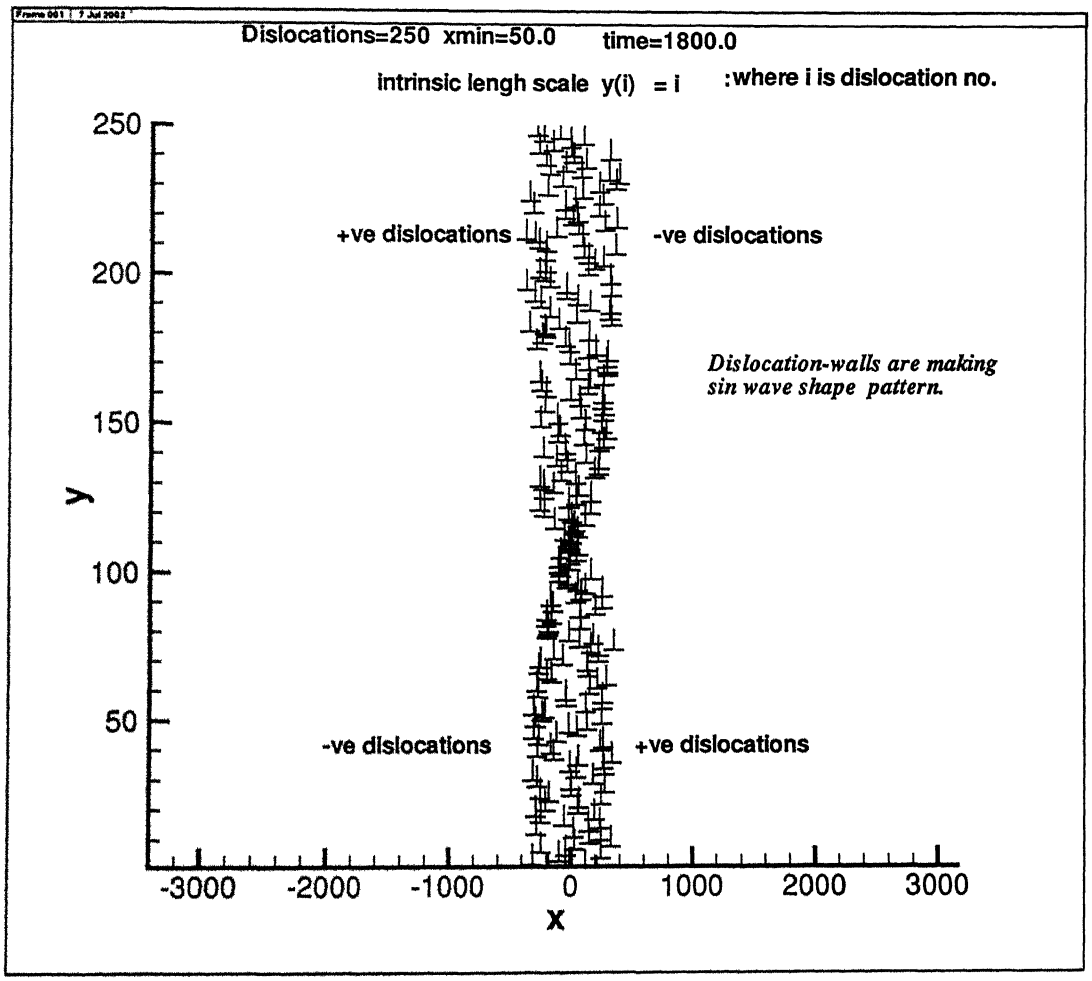

Figure 5.8a: Many Dislocations clustering with time: with diffrent intrinsic lengh scale

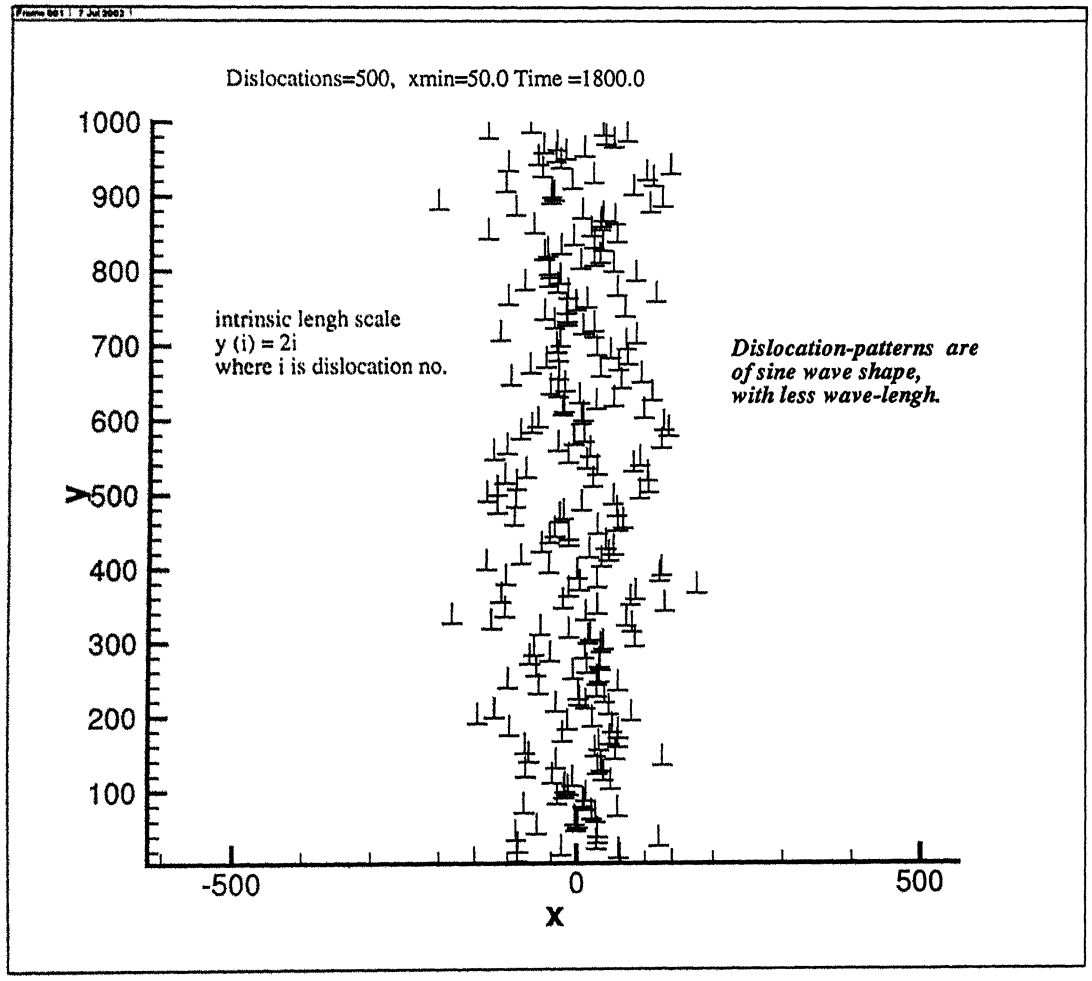

Figure 5.8b: Many Dislocations clustering with time: with different intrinsic lengh scale

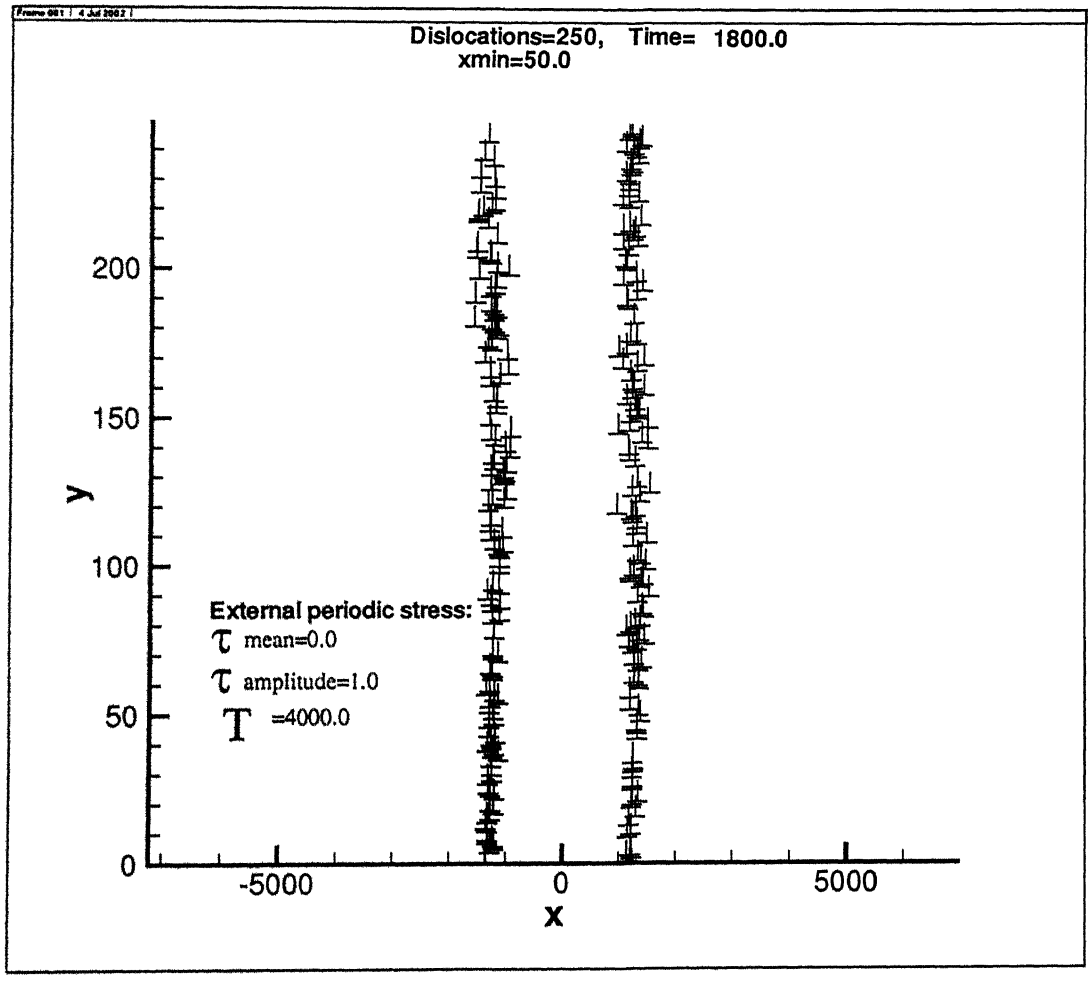

Figure 5.9a: Dislocation Distribution:External Stress

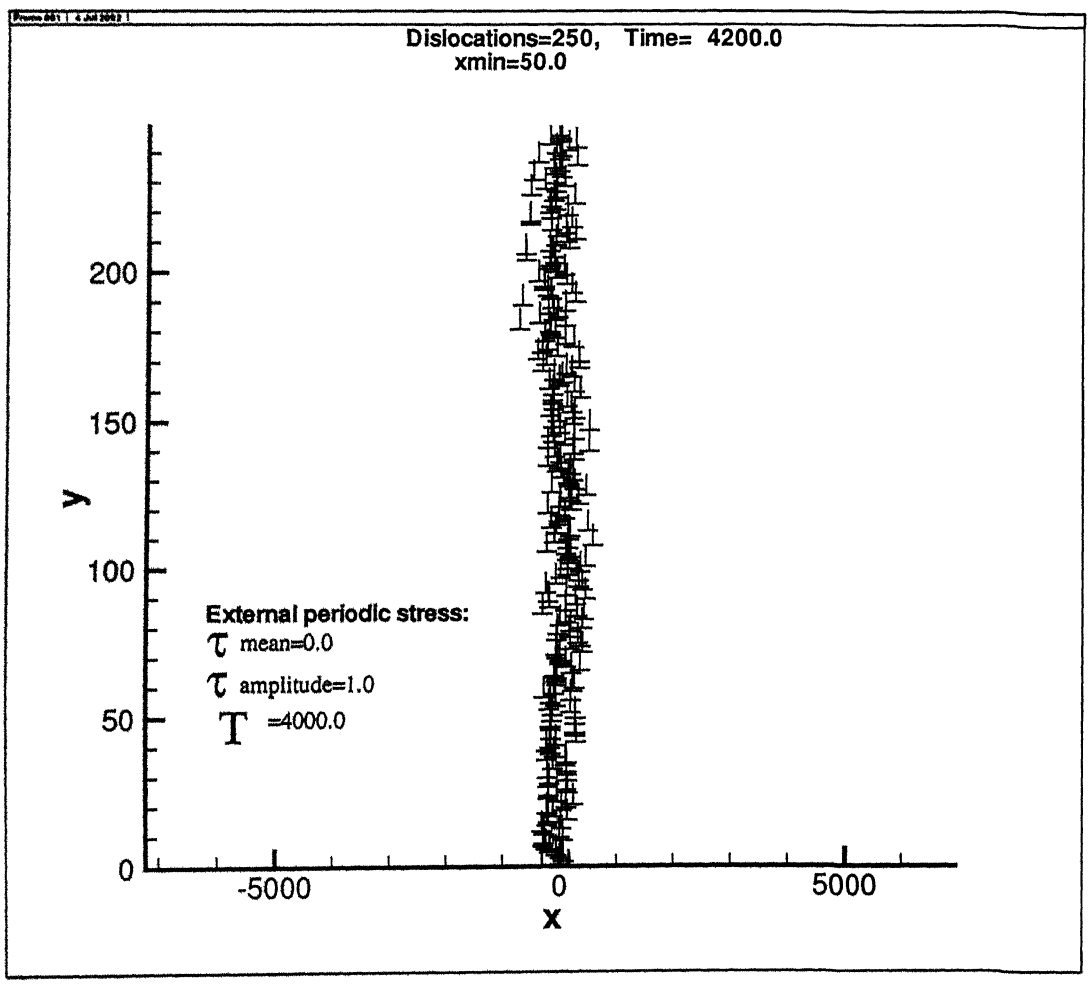

Figure 5.9b: Dislocation Distribution:External Stress

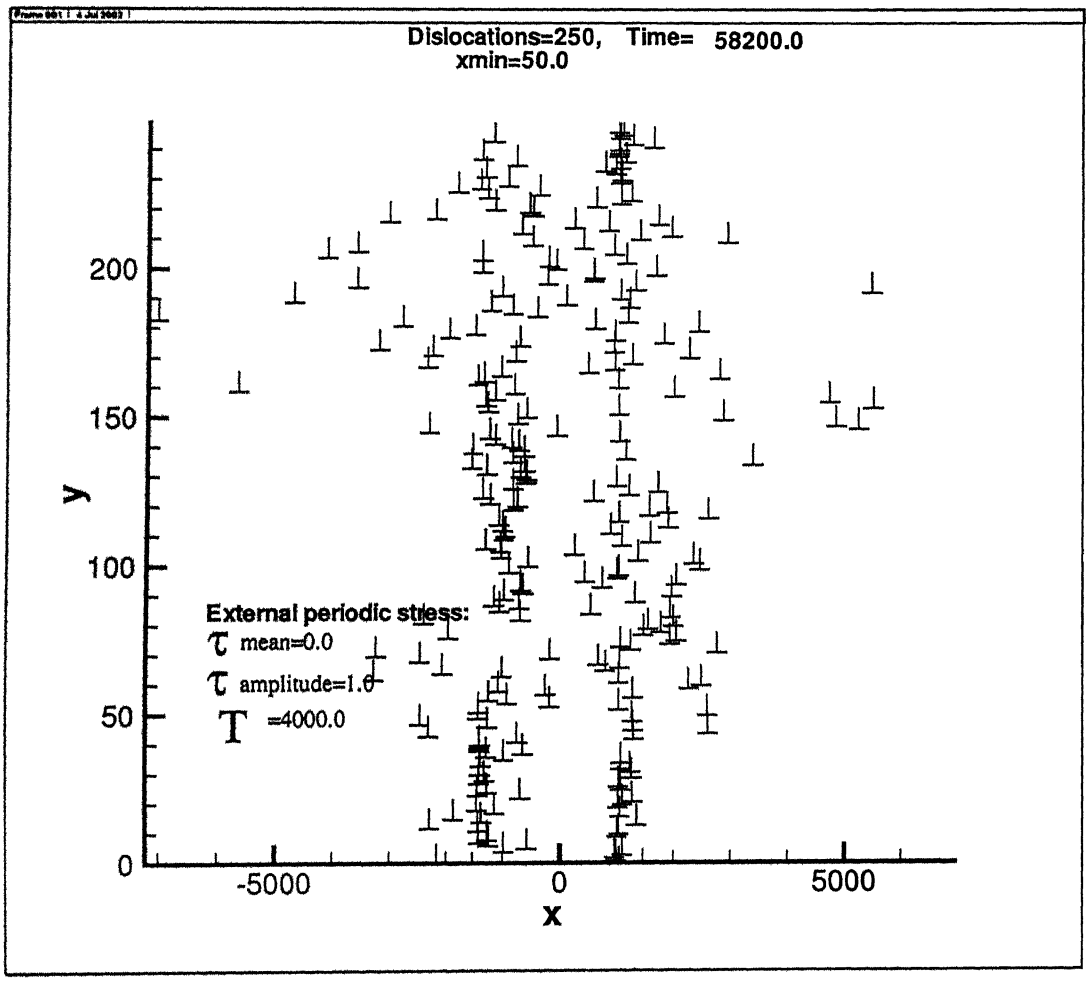

Figure 5.9c: Dislocation Distribution:External Stress

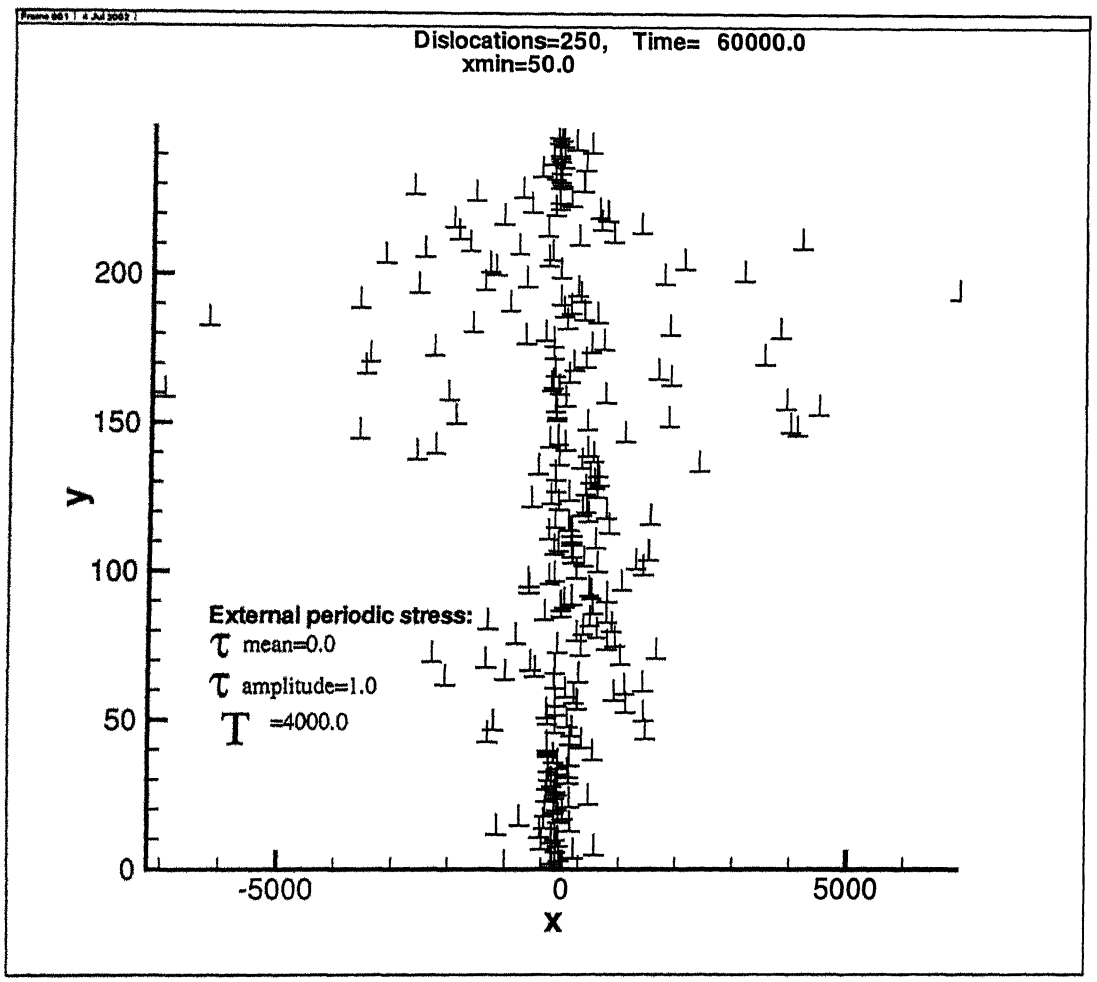

Figure 5.9d: Dislocation Distribution:External Stress

Chapter 6

Conclusion

6.1 Conclusion

In the present study, the dislocations for one dimensional and two dimensional are being studied in case of applying external shear stresses. The unit edge dislocations are being studied for only their gliding in their slip planes.the distribution of dislocations by internal stress finally, is very surprising in case of two-dimensional distributed dislocations.
Some important conclusions may be pointed out as following:

1. In case of two dislocations in a line the dislocations are attracting towards each other till they annihilate .

    - The dislocation glide is prominently influenced by the external stresses ,the gliding of dislocation is vibrated on x-axis by periodicity of external stress, if the amplitude and periodicity of cyclic stress is high.
    - When the external stress is of low periodicity and low amplitude the vibration is very low, when the amplitude is increased the dislocation vibrates with high amplitude in the same frequency. But the same time both dislocations move continually towards each other till time for annihilation.
    - When the dislocations move beyond the time of annihilation (in our case that is unit), the dislocation shows mini-vibrations except the

periodicity by external stress. This vibration is due to iteration of $1/2x$ of equation 3.16, which fails to converge after annihilation time.

2. In case of n dislocations in a line the resultant stress field is such that one positive dislocation moves to $+\infty$ and one negative dislocation moves to $-\infty$. remaining dislocations vibrates around their initial coordinates.

3. In case of n dislocations on two-dimensional field they make two vertical clusters of of positive dislocations and negative dislocations which move with time away from each other.we have seen from section(2.5) that the dislocations are stable when $\pm x = 0$, so they make clusters of same sign dislocations.

   - The vertical walls move away from each other with time. This is due to the fact that the net elastic energy can be reduced if they form walls and move away from each other. We can understand this from the fact the the forces acting on the dislocations from the other dislocations can be thought of as the derivative of the interaction energy of the two dislocations.
   - If the *xmin* is increased successively, the dislocation wall tend to defuse.We can understand this as, if the same no. of dislocations are distributed on larger field then the resultant stress field is not so intense to generate the regular pattern.
   - If there is no intrinsic length scale, then the walls separate out to the left and right. If there is indeed an intrinsic length scale then we see that the wall splits into the form of a sin wave. But if we make the length of the simulation cell in the y direction longer, the wavelength of the wave is also larger. What this means is that if the simulation cell size is much larger compared to the intrinsic length scale, then we see two walls to the left and right.
   - we can use this to explain the patterns observed in experiments. If the dislocation density is large, then the intrinsic length scale is important. Thus we will see the dislocations going into small pockets rather than

walls as we see in the simulations with a length scale. Thus, qualitatively what we see in the simulations is in over all agreement with experiments.

4. In case of external stress the dislocation-walls are driven by external stress, they vibrate with time on x-axis.The dislocation-walls deteriorate with time also.

6.2 Scope for Future Work

1. In the present study, we have considered only the external cyclic stress of pure shear type, we can also consider the different type of loads like compressive ,tensile and mixed state of all these.

2. In the whole study we have considered only pure edge dislocations. We have scope for doing this simulation for pure screw dislocations and mixed dislocations also.

3. In case of two-dimensional simulation we have neglected the inter-slip motion of dislocation, So we neglected the force in y direction. We can include climb for further study.

4. We have not included the annihilation in our *computer-code*, The code can be modified for annihilation.

5. If very powerful computational system is available then three-dimensional simulation which is more realistic, can be done.

Bibliography

[1] A N Gullouglu and C S Hartley *Simulation of dislocaion microstructures in two dimensions:Dynamic and relaxed strucyures* Department of mechanical Engineering,College of Engineering,Florida Atlantic University,Boca Raton,FL 33431, USA

[2] Mughrabi H *Plastic Deformation and Fracture of Materials* 1993 VCH Germany

[3] Hull D and Bacon D J 1984 *Introduction to Dislocations* 3rd edition(Newyork: Pergamon)

[4] Vitek V 1974 *Cryst.Lattice Defects*

[5] Gould H and Tobochnik J 1988 *Introduction to computer simulation Methods Application to physical systems* (New York: Addison-Wisly)

[6] J L Sokolnikoff *The Mathematical Theory of Elasticity* McGraw-Hill,New York,1956

[7] Mughrabi H 1975 *constitutive equations in plasticity*(Cambridge ,MA:MIT Press) p 199

[8] Cottrell A H 1953 *Didslocations and Plastic Flow in Crystals*(Oxford :Oxford University Press) p 98

[9] Hirth J P and Lothe J 1968 *Theory of Dislocations*(New York: McGraw-Hill)

[10] Gulloglu A N 1991 Computer simulation of dislocation microstructures *Ph D Dissertation* University of Alamba at Birmingham

[11] Martyn J L and Argon A S 1986 *Low Energy Dislocation Structures*ed M N Basin (Lussane: Elsevier Sequoia) p 337.

[12] Gulloglu A N and Hartley C S 1992 *Modelling Simulation in Material Science* 1

[13] Muragbi M 1975 *Constitutive Equations in Plasticity* edition A S Argon (Cambridge,MA: MIT Press) p 251